CANCER IMMUNOTHERAPY

A T cell receptor β chain–directed antibody fusion molecule activates and expands subsets of T cells to promote antitumor activity

Jonathan Hsu[1]†, Renee N. Donahue[2]†, Madan Katragadda[1], Jessica Lowry[1], Wei Huang[1], Karunya Srinivasan[1], Gurkan Guntas[1], Jian Tang[1], Roya Servattalab[1], Jacques Moisan[1], Yo-Ting Tsai[2], Allart Stoop[1], Sangeetha Palakurthi[1], Raj Chopra[1], Ke Liu[1], E. John Wherry[3,4], Zhen Su[1], James L. Gulley[2], Andrew Bayliffe[1]*†, Jeffrey Schlom[2]*†

Despite the success of programmed cell death-1 (PD-1) and PD-1 ligand (PD-L1) inhibitors in treating solid tumors, only a proportion of patients respond. Here, we describe a first-in-class bifunctional therapeutic molecule, STAR0602, that comprises an antibody targeting germline Vβ6 and Vβ10 T cell receptors (TCRs) fused to human interleukin-2 (IL-2) and simultaneously engages a nonclonal mode of TCR activation with costimulation to promote activation and expansion of αβ T cell subsets expressing distinct variable β (Vβ) TCR chains. In solution, STAR0602 binds IL-2 receptors in cis with Vβ6/Vβ10 TCRs on the same T cell, promoting expansion of human Vβ6 and Vβ10 CD4$^+$ and CD8$^+$ T cells that acquire an atypical central memory phenotype. Monotherapy with a mouse surrogate molecule induced durable tumor regression across six murine solid tumor models, including several refractory to anti–PD-1. Analysis of murine tumor-infiltrating lymphocyte (TIL) transcriptomes revealed that expanded Vβ T cells acquired a distinct effector memory phenotype with suppression of genes associated with T cell exhaustion and TCR signaling repression. Sequencing of TIL TCRs also revealed an increased T cell repertoire diversity within targeted Vβ T cell subsets, suggesting clonal revival of tumor T cell responses. These immunological and antitumor effects in mice were recapitulated in studies of STAR0602 in nonhuman primates and human ex vivo models, wherein STAR0602 boosted human antigen-specific T cell responses and killing of tumor organoids. Thus, STAR0602 represents a distinct class of T cell–activating molecules with the potential to deliver enhanced antitumor activity in checkpoint inhibitor–refractory settings.

INTRODUCTION

T cells play a central role in immune responses to cancer as evidenced by the clinical activity of antibody therapies targeting immune checkpoints, such as cytotoxic T lymphocyte–associated protein 4 (CTLA-4) and programmed cell death protein 1 (PD-1) (*1*), and the treatment of hematological malignancies with T cell engagers and adoptive T cell therapies (*2*, *3*). Despite these encouraging results, treatment of solid tumors with T cell–directed therapies has limitations (*4*), and most patients fail to respond or progress after checkpoint inhibitor (CPI) treatment (*5*). Correlates of response to CPIs in solid tumors converge on factors associated with tumor immunogenicity and T cell activity (*6*), such as tumor mutation burden (TMB), degree of T cell infiltration, interferon-γ (IFN-γ) signatures, and PD-1 ligand (PD-L1) expression (*7*, *8*). Therefore, to enhance immunotherapy in patients with solid tumors, including those with low T cell infiltration and neoantigen burden (immunologically "cold" tumors), there is an urgent need to develop therapies that improve the quantity and quality of T cell responses to augment a successful antitumor immune response.

Foremost among the interactions that govern T cell recognition and killing of cellular targets is the recognition and binding of peptides presented to the T cell receptor (TCR) comprising the variable α and β chains. TCR αβ heterodimers lack their own signaling domain and interact with CD3 ε, γ, δ, and ζ subunits and CD4 or CD8 co-receptors to mediate the primary T cell activation signal ("signal 1"). T cell activation and proliferation are further enhanced through the engagement of costimulatory receptors such as CD28 ("signal 2") and cytokines ("signal 3") (*9*). The affinity and avidity of TCR engagement exerts a strong influence on fate commitment of peripheral T cells and whether they mature into short-lived effectors, acquire durable systemic or tissue-resident memory phenotypes, or differentiate to become an exhausted lineage of cells (*10*). However, attempts to artificially stimulate αβ T cells through the TCR complex using agonist anti-CD3 antibodies that activate all T cells frequently result in massive cytokine release, activation of predominantly short-lived effector T cells, and exhaustion of residual T cells. None of these effects is desirable in the setting of tumor immunotherapy, and therefore investigation of alternative mechanisms that activate T cells through the TCR is warranted.

Although the TCR generates clonal responses to diverse peptide antigens predominantly through the hypervariable complementarity determining region 3 (CDR3), the foundation of human TCR repertoire diversity is created by polymorphic CDR1 and CDR2 domains within the germline-encoded repertoire of Vα and Vβ genes. Of the 48 Vβ genes in humans, approximately 30 are functional and define the "germline TCR repertoire" of T cell subsets that exist at varying frequencies ranging from about 0.1% to

[1]Marengo Therapeutics, Cambridge, MA 02139, USA. [2]Center for Immuno-Oncology, Center for Cancer Research, National Cancer Institute, NIH, Bethesda, MD 20892, USA. [3]Department of Systems Pharmacology and Translational Therapeutics, University of Pennsylvania, Philadelphia, PA 19104, USA. [4]Institute for Immunology, University of Pennsylvania, Philadelphia, PA 19104, USA.
*Corresponding author: abayliffe@marengotx.com (A.B.); schlomj@mail.nih.gov (J.S.)
†These authors contributed equally to this work.

about 10% of T cells. Sequencing of TCRs in tumor-infiltrating lymphocytes (TILs) across diverse cancers suggests that the most frequently used Vβ genes (e.g., TRBV20-1, TRBV5-1, and TRBV6-5) define T cell subsets that exist in both TILs and circulating T cells at frequencies of 6 to 10% and are common to all cancers (*11*).

Whereas the TCR is generally considered an adaptive modality, αβ TCRs can also act as an innate receptor, engaging nonclonal ligands at germline-encoded sites (*12*). This is the case for superantigen (SAg) proteins expressed by some bacteria and viruses that bind to specific germline-encoded Vβ sequences, driving potent activation and proliferation of subsets of Vβ T cells. Previously, purified SAgs (*13*) and fusion proteins that target SAgs to tumor cells have shown antitumor activity in animal models as a result of the activation and expansion of distinct germline Vβ T cell subsets (*14*). However, the therapeutic utility of SAgs in humans is limited by the risk of overactivation of T cells, in addition to the rapid development of neutralizing antibody responses to these highly immunogenic proteins (*15*).

Here, we describe the design and testing of a fully human bifunctional antibody fusion molecule (STAR0602) comprising an antibody that binds the germline Vβ6 and Vβ10 TCRs of human αβ T cells fused with a native human interleukin-2 (IL-2) cytokine molecule. In chronic infection models, native IL-2 [and not IL-2 muteins with reduced binding to IL-2 receptor (IL-2R) α (CD25)] drives the development of $CD8^+$ T cells with high effector potentials in a CD25-dependent manner (*16*). Moreover, in vitro stimulation of human T cells with anti-Vβ6/Vβ10 antibodies also promotes induction of CD25 (*17*). Thus, by fusing an anti-Vβ6/Vβ10 antibody to a native IL-2 molecule, STAR0602 achieves selective activation and expansion of $CD8^+$ and $CD4^+$ Vβ6/Vβ10 T cells by simultaneously engaging a distinct mode of TCR activation with IL-2R binding and activation in cis on the same cell. STAR0602 and a murine surrogate molecule showed potent single-agent antitumor activity in multiple CPI-refractory human organoid tumor and murine syngeneic models with acceptable tolerability and limited cytokine release in monkeys and mice. Durable antitumor responses, with long-term protection from tumor rechallenge, were associated with de novo expansion and tumor infiltration of targeted Vβ T cell subsets with an effector memory gene signature and an increase in CDR3 repertoire diversity. Collectively, these data support the potential of STAR0602 to drive robust T cell responses to solid tumors through a distinct mechanism of action to CPIs, which may offer a safe and effective therapy for patients who have progressed after CPI treatment.

RESULTS

STAR0602 binding is selective for Vβ6/Vβ10 T cell subsets

On the basis of publicly available data, we chose to target the Vβ6 TCR T cell subset because it exists at a high prevalence relative to other Vβ subsets in TILs and is common across all cancers (*11*). To confirm this finding at the protein level, we assessed the prevalence of Vβ6-5 TCRs (the most common member of the Vβ6 family) in TILs from primary tissue collected from patients with a range of solid tumors. As measured by flow cytometry, Vβ6-5 T cells comprised between 2 and 8% of TILs across tested tumors, with similar frequencies observed in donor-matched peripheral blood mononuclear cells (PBMCs) and healthy donor PBMCs (Fig. 1A). On the basis of this finding, we designed STAR0602 as a bifunctional antibody fusion molecule comprising an affinity-matured anti–Vβ6-5 Fab and a native IL-2 molecule fused by its C terminus to the Fc domain (Fig. 1B). The immunoglobulin G1 (IgG1) Fc domain of STAR0602 contains knob-in-hole mutations to promote Fc heterodimerization and an N297A mutation to abrogate effector functions.

Using a surface plasmon resonance (SPR) binding assay, STAR0602 binds with high affinity [dissociation constant (K_D)] to purified human Vβ6-5 (1.7 nM), IL-2Rα (45 nM), IL-2Rβγ (3.8 nM), and the high-affinity trimeric IL-2R (0.1 nM), which is similar to the affinity of both recombinant human IL-2 (rhIL-2) and the "in-format" anti–RSV–IL-2 Fab control molecule (IL-2 control) for the IL-2R subunit chains (table S1). Using flow cytometry, we confirmed that STAR0602 binds to $CD4^+$ and $CD8^+$ T cells and affinities for both cell types were similar, with a half-maximal effective concentration (EC_{50}) of 0.21 ± 0.03 nM in $CD4^+$ T cells and 0.52 ± 0.2 nM in $CD8^+$ T cells (Fig. 1C). Low expression of IL-2R on naïve T cells prohibits accurate cellular IL-2 binding studies; however, in a cellular assay of IL-2 bioactivity using the detection of phosphorylated signal transducer and activator of transcription 5 (pSTAT5), both STAR0602 and the IL-2 control molecule showed attenuated (100-fold lower) IL-2 bioactivity compared with rhIL-2 (Fig. 1D). These data suggest that presentation of the IL-2 moiety in the bifunctional STAR0602 format contributes to a reduction in its bioactivity, possibly due to steric hinderance in binding of IL-2 to its cognate receptors.

To further explore the mode of STAR0602 binding, four human T cell populations were created in vitro using a combination of flow cytometry sorting methods and cycles of T cell stimulation and rest to generate populations of cells with contrasting amounts of STAR0602 target expression corresponding to the extremes of possible $Vβ6\text{-}5^+$ and $CD25^+$ T cell frequencies (fig. S1A). Binding of STAR0602 to these manipulated T cell populations over a wide concentration range was then measured at a single-cell level using flow cytometry. In untreated T cells isolated from healthy human donors, STAR0602 bound to 3 to 5% of T cells over a pharmacologically relevant concentration range, reflecting binding to the expected proportion of Vβ6-5 T cells in a physiologically normal state (Fig. 1E). In manipulated T cell populations comprising 98% Vβ6-5 T cells, STAR0602 bound to both $CD25^{low}$ and $CD25^{high}$ cells, with higher affinity binding to $CD25^{high}$ Vβ6-5 T cells (1.3 nM) compared with $CD25^{low}$ Vβ6-5 T cells (10 nM). In unsorted, in vitro stimulated T cells comprising 3 to 5% Vβ6-5 T cells and >98% $CD25^{high}$ T cells (an uncommon state for the human T cell compartment), STAR0602 bound with much lower affinity (62 nM). Furthermore, when we evaluated STAR0602 binding to established T cell lines that exclusively coexpress CD25 and either Vβ6-5 (P12-Ichikawa) or an unrelated Vβ chain TCR (HSB-2 cells expressing Vβ5-1) (fig. S1B), STAR0602 bound only to the Vβ6-5 P12-Ichikawa cells, whereas HSB-2 cells showed minimal to no binding (fig. S1C). Collectively, these data suggest that STAR0602 preferentially binds its targets in cis on the same cell in an anti-Vβ–dependent manner with higher affinity to T cells that coexpress Vβ6-5 and IL-2R, possibly due to a higher avidity interaction on these cells.

Finally, to assess the functional selectivity of STAR0602, PBMCs from healthy donors were stimulated in vitro with STAR0602, and the relative abundance of all Vβ T cell subsets was assessed by TCR sequencing. Among the 48 known germline-encoded Vβ chains, STAR0602 promoted the expansion of predominantly Vβ6 T cell

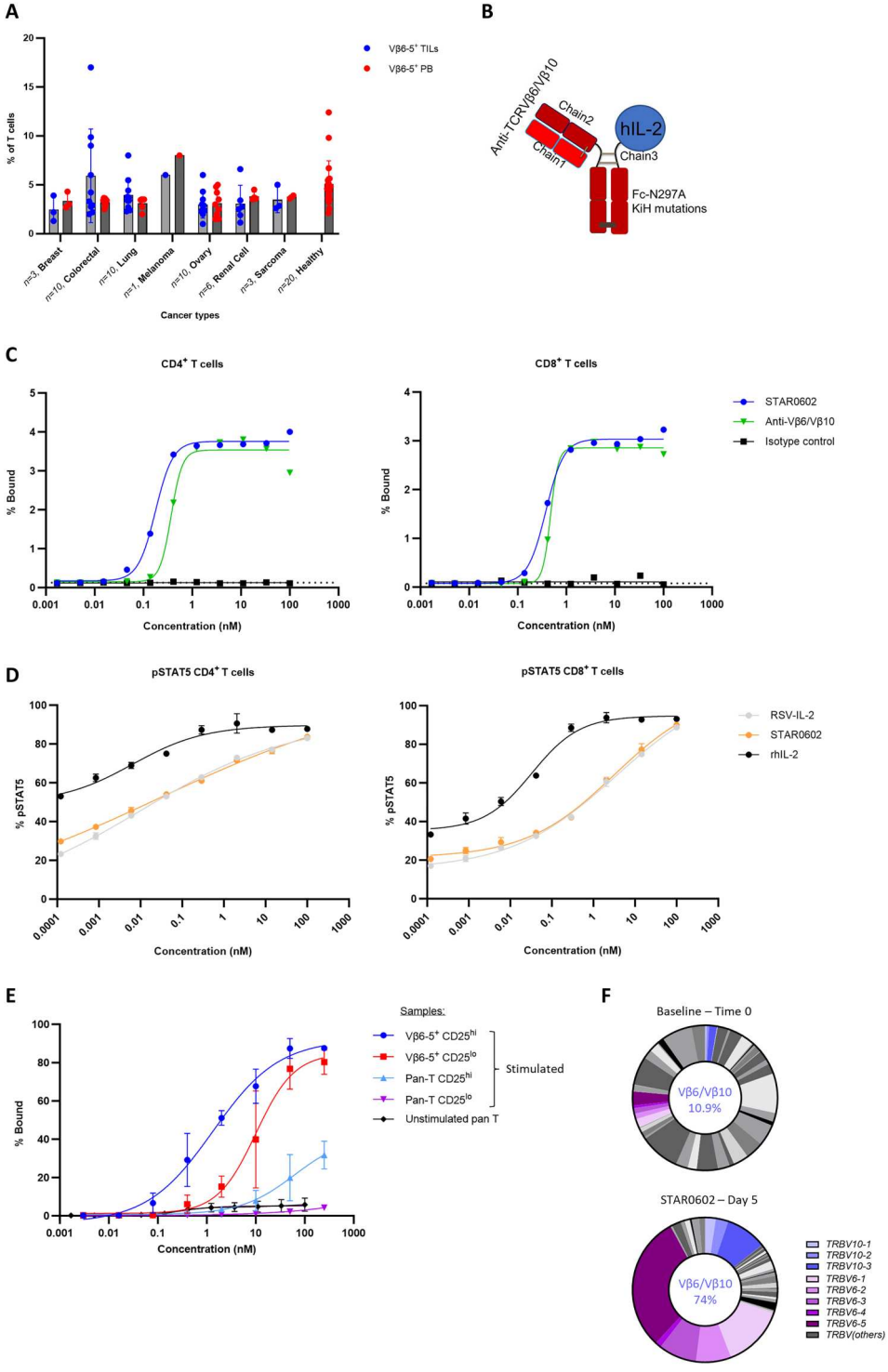

Fig. 1. Vβ6-5 T cells are detected in TILs, and STAR0602 binds with high affinity and selectivity in human T cells. (**A**) Prevalence of Vβ6 TCR T cells in isolated TILs and PBMCs from patients with cancer ($n = 43$) and from healthy donor PBMCs ($n = 20$, data are presented as mean ± SEM). (**B**) Schematic of STAR0602. (**C**) Binding curves for STAR0602 and control molecules to human $CD4^+$ and $CD8^+$ T cells (representative donor of $n = 3$). (**D**) pSTAT5 activity comparing IL-2 bioactivity for STAR0602, RSV-IL-2 control, and rhIL-2 (representative donor of $n = 3$, data are presented as mean ± SEM of technical duplicates). (**E**) STAR0602 binding to unstimulated and stimulated-sorted T cell populations (pan-T cells or Vβ6-5–sorted T cells comprising either high or low expression of CD25 after anti-CD3/CD28 stimulation or resting of cells, respectively) (representative donor of $n = 3$, data are presented as mean ± SEM of technical triplicates). (**F**) Pie chart of relative frequencies of human T cell Vβ6 (purple)– and Vβ10 (blue)–encoding transcripts before and after in vitro stimulation with STAR0602 at 10 nM ($n = 3$, data are presented as mean). Experiments in (E) and (F) were performed two times with similar results.

subsets (expressing *TRBV6-1*, *6-2*, *6-3*, *6-4*, and *6-5* gene transcripts), in addition to some limited expansion of Vβ10 T cells (expressing *TRBV10-1*, *10-2*, and *10-3* gene transcripts) (Fig. 1F and fig. S2), reflecting the close sequence homology between these two V gene families. However, STAR0602 predominantly expands Vβ6 T cells, with this subset comprising >60% of T cells after STAR0602 stimulation, suggesting selectivity for Vβ6 TCRs.

STAR0602 activates and expands Vβ6/Vβ10 T cells with a central memory phenotype

Next, the kinetics of in vitro human Vβ6/Vβ10 T cell expansion by STAR0602 was investigated by enumerating Vβ6/Vβ10 T cells using flow cytometry. In healthy donor PBMCs, Vβ6 T cells comprise on average 5.2% of $CD4^+$ T cells, 6.8% of $CD8^+$ T cells, and 5.6% of $CD4^+$ $FoxP3^+$ regulatory T cells (T_{regs}) (table S2). As shown in Fig. 2A, Vβ6/Vβ10 T cells incrementally increased over time with frequencies rising from a baseline of 9% of T cells to 27%, 38%, 47%, 50%, and 52% on days 4, 5, 6, 7, and 8, respectively, after stimulation. The magnitude of in vitro activation of both $CD4^+$ and $CD8^+$ T cells by STAR0602 was concentration dependent (Fig. 2B), although differences in EC_{50} values (5.16 ± 6.04 nM for $CD4^+$ T cells and 1.98 ± 1.81 nM for $CD8^+$ T cells) suggest preferential activation of $CD8^+$ over $CD4^+$ T cells (table S3). Control molecules showed minimal to no activation of T cells. To further investigate differential in vitro expansion of human $CD8^+$ versus $CD4^+$ T cells, cell counts normalized to unstimulated samples were compared from the same donor. Here, STAR0602 increased the number of $CD8^+$ T cells to a threefold greater extent than $CD4^+$ T cells, although the magnitude of this effect varied across donors (Fig. 2C). Thus, although both $CD4^+$ and $CD8^+$ T cells are activated by STAR0602, the expansion of $CD8^+$ T cells is more pronounced. To explore whether this expansion and activation of T cells is dependent on engagement of both arms of STAR0602, purified T cells were incubated for 5 days with a fixed concentration of STAR0602 (10 nM) and increasing amounts of competing soluble IL-2R, Vβ6-5 antigen, or a mixture of both. The addition of these competitors elicited a dose-dependent inhibition of T cell activation (as measured by acquisition of CD25 expression) and expansion (fig. S3), suggesting that both arms of STAR0602 are required for activity.

Antibody-induced TCR activation generally requires receptor clustering and cross-linking using a solid support. In an earlier study (*18*), treatment of human PBMCs or purified T cells with plate-coated anti-Vβ antibodies was shown to induce expansion of Vβ6/Vβ10 $CD8^+$ T cells with a central memory ($CD95^+$ $CCR7^+$ $CD45RA^-$) T cell phenotype (T_{CM}). Here, we show that STAR0602 in solution (not presented on a solid surface) recapitulates this T_{CM} phenotype, presumably by orchestrating coclustering of TCRs with IL-2Rs on the surface of Vβ6 and Vβ10 T cells (Fig. 2D). This shift to a T_{CM} phenotype was consistently observed in both $CD4^+$ and $CD8^+$ T cells across multiple donors (Fig. 2E) and was not observed for control molecules (anti-Vβ6/Vβ10 monovalent Fab or IL-2 control) in solution.

To confirm that STAR0602 activates signaling pathways downstream of both the TCR and IL-2R, phosphorylated extracellular signal–regulated kinase (pERK), phosphorylated SH2 domain–containing leukocyte protein of 76 kDa (pSLP76), and pSTAT5 (proximal regulators of TCR and IL-2 signaling) were measured from cellular lysates. In STAR0602-stimulated human $CD8^+$ T cells, pERK was increased 3.9-fold, and pSLP76 (Tyr^{145}) was 2.1-fold higher than control molecules (Fig. 2F). In these experiments, plate-coated anti-Vβ6/Vβ10 Fab (no IL-2) also activated pERK and pSLP76 to similar degrees as STAR0602 in solution, confirming the specificity of these markers for Vβ6/Vβ10 TCR activation and implicating TCR clustering as an important component of STAR0602 mechanism of action. Finally, pSTAT5 was increased up to 20-fold after treatment with STAR0602 and the IL-2 control molecule, but not by the anti-Vβ6/Vβ10 monovalent antibody, either in solution or when plate-coated (overlapping curves in Fig. 2F). Consistent with the impact of plate-coated anti-Vβ6/Vβ10 Fab on primary T cells (*18*), we observed a marked up-regulation of cells coexpressing CD25, intracellular granzyme B, and IFN-γ in STAR0602-stimulated human $CD8^+$ T cells, implying that STAR0602 induces an atypical T_{CM} phenotype with concomitant expression of cytotoxic effector molecules (Fig. 2G).

mSTAR1302 promotes antitumor activity across multiple murine syngeneic tumor models

Because a homolog of the Vβ6 gene does not exist in mice, a surrogate molecule (mSTAR1302) comprising the same human IL-2 antibody fusion design as STAR0602 and that targets and expands the most abundant murine Vβ T cell subset (Vβ13) was developed. Consistent with in vitro assessments of STAR0602 in human PBMCs, in vitro stimulation of mouse splenocytes with mSTAR1302 resulted in the activation and expansion of both $CD4^+$ and $CD8^+$ Vβ13 T cells in a concentration-dependent manner (fig. S4A), with similar potency to STAR0602 (EC_{50}, 12 ± 13 nM for $CD4^+$ T cells and 0.4 ± 0.6 nM for $CD8^+$ T cells).

After administration of a single intraperitoneal dose in BALB/c mice, mSTAR1302 showed rapid clearance in serum (fig. S4B) yet induced robust expansion of Vβ13 $CD8^+$ T cells and, to a lesser extent, Vβ13 $CD4^+$ T cells in peripheral blood, without expanding T_{regs} (fig. S4C). Additional details of mSTAR1302 pharmacokinetics are shown in table S4. In BALB/c EMT6 tumor–bearing mice, mSTAR1302 distributed extensively into peripheral tissues, including tumor, spleen, liver, kidney, and lung tissue, up to 48 hours after dosing (fig. S4D).

To investigate the potential for idiosyncratic IL-2–mediated toxicity, such as vascular inflammation and injury, BALB/c mice were dosed weekly with mSTAR1302 (0.5 to 1.5 mg/kg, intraperitoneally) or phosphate-buffered saline (PBS), or rhIL-2 at a dose regimen designed (*19*) to recapitulate high-dose aldesleukin use in humans (a 9-day course of 8 mg/kg twice daily rhIL-2). In blood, targeted Vβ13 $CD8^+$ T cells were expanded in mice dosed with mSTAR1302 (fig. S5A) but not with PBS or rhIL-2. In the lungs and livers of mice dosed with rhIL-2, pronounced perivascular leukocytic infiltration was observed surrounding sinusoidal liver vessels and pulmonary vessels (fig. S5, B and C), consistent with early signs of vascular injury (*19*). Similar to the effects of aldesleukin in humans, mice dosed with rhIL-2 also showed changes in liver enzyme markers of hepatic injury (fig. S5D). In contrast, no perivascular inflammation or liver enzyme changes were observed in mice administered mSTAR1302 once per week at doses up to and including 1.5 mg/kg. This is reassuring because the optimal efficacious mSTAR1302 dose in tumor-bearing mice was demonstrated to be 1 mg/kg weekly (fig. S6A).

The antitumor activity of mSTAR1302 was assessed in six murine syngeneic solid tumor models with differing degrees of T

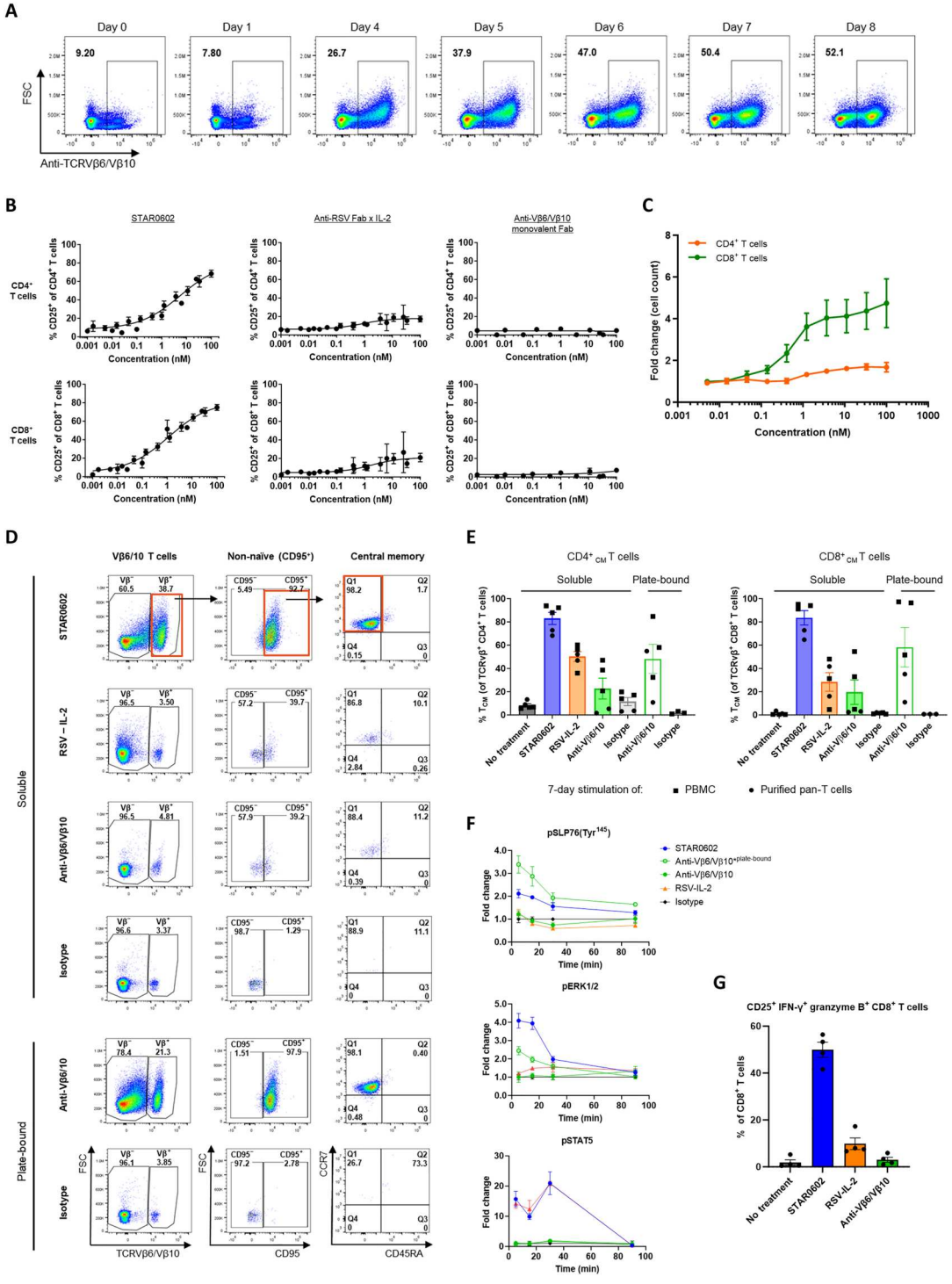

Fig. 2. STAR0602 activates Vβ6/Vβ10 T cells in vitro with preferential expansion of CD8$^+$ T cells with an atypical central memory–like phenotype. (**A**) Expansion of human Vβ6/Vβ10 T cells with 10 nM STAR0602 over 8 days (representative donor of $n = 3$). FSC, forward scatter. (**B**) Activation (CD25$^+$) of human CD4$^+$ (top) and CD8$^+$ (bottom) T cells after a 5-day stimulation with STAR0602 ($n = 20$, data are presented as mean ± SEM) or controls. (**C**) Direct cell counts of human CD4$^+$ and CD8$^+$ T cells after a 5-day stimulation with STAR0602 (10 nM) ($n = 4$, data are presented as mean ± SEM). (**D**) Representative flow cytometry plots showing the differentiation of Vβ6/Vβ10 CD8$^+$ T cells to a central memory (CD95$^+$ CD45RA$^-$CCR7$^+$) phenotype after a 7-day culture with STAR0602 (10 nM) or controls. (**E**) Summary analysis for CD4$^+$ (left) and CD8$^+$ (right) Vβ6/Vβ10 central memory T cells as a percentage of total Vβ6/Vβ10 T cells in (D); $n = 5$, data are presented as mean ± SEM. (**F**) Assessment of TCR and IL-2R signaling in purified CD8$^+$ T cells stimulated with STAR0602 or controls by quantifying pSLP76, pERK, and pSTAT5 (representative donor of $n = 3$, data are presented as mean ± SEM of technical replicates). (**G**) Percentage CD25$^+$, IFN-γ$^+$, and granzyme B$^+$ triple-positive CD8$^+$ T cell subsets by flow cytometry after a 5-day stimulation with STAR0602 (10 nM) or controls; $n = 4$, data are presented as mean ± SEM. Experiments in (B) are from six independent studies, and those in (C) and (E) are from two studies. Experiments in (G) were performed two times with similar results.

cell infiltration, different tumor microenvironment (TME) conditions, and varying responsiveness to CPI therapy (*20*). In dose-finding studies of mSTAR1302 in the EMT6 breast cancer model, four consecutive 1 mg/kg doses given once weekly were determined as optimal in relation to antitumor activity (fig. S6A); however, in subsequent scheduling studies, just a single 1 mg/kg dose of mSTAR1302 was shown to elicit similar tumor regression (fig. S6B).

In mice treated with mSTAR1302 as a single agent, tumor growth inhibition was observed in all six syngeneic models, with complete tumor regression in the EMT6 model. Tumor growth inhibition compared with the PBS-treated group was calculated to be 98% in CT26 (day 24, a time point where the tumors from the PBS group exceed 2000 mm^3), 70% in MC38 (day 17), 66% in RENCA (day 20), 57% in RM1 (day 12), and 86% in the highly refractory

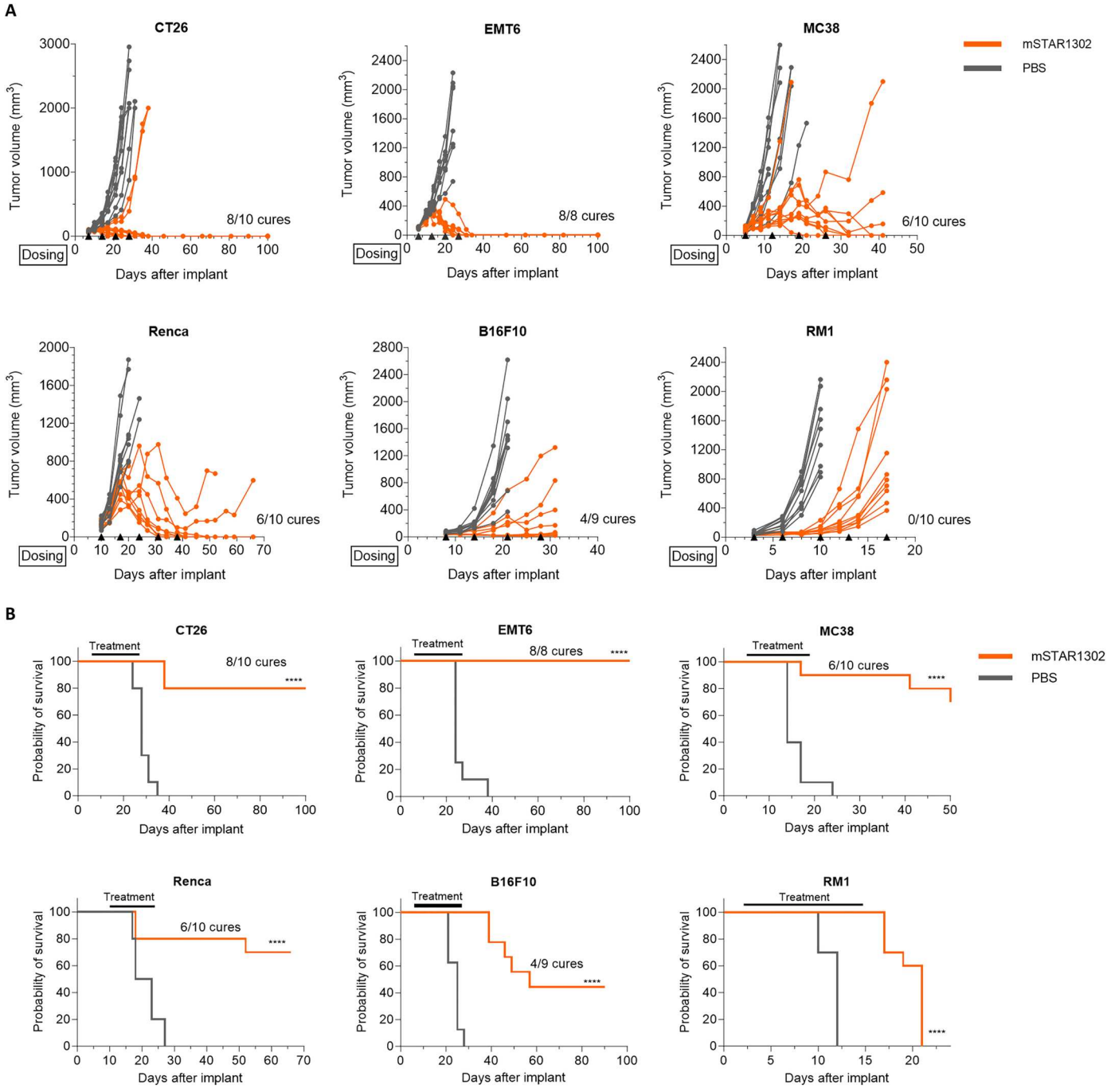

Fig. 3. mSTAR1302 induces tumor regression and survival across multiple murine syngeneic solid tumor models. (**A**) Tumor cell lines were implanted by subcutaneous injection. When tumors reached 80 to 150 mm^3, four or five intraperitoneal doses of mSTAR1302 were administered at a concentration of 1 mg/kg (CT26, EMT6, B16F10, MC38, and Renca) once weekly or 1.5 mg/kg (RM1) twice weekly. The individual tumor volumes were monitored by caliper measurements over time to a threshold of 2000 mm^3, which was the study endpoint; $n = 8$ to 10 mice per group as indicated. Arrowheads indicate dosing days. (**B**) Survival curve for each tumor model. Significance was measured by log-rank Mantel-Cox test (****$P < 0.0001$). Studies with CT26 and EMT6 were performed three times, and those with MC38 and B16F10 were performed two times with similar results.

B16F10 model (day 21) (Fig. 3A). The antitumor activity of mSTAR1302 also increased survival in all six tumor models evaluated (Fig. 3B). The activity of mSTAR1302 was directly compared with a mouse anti–PD-1 antibody in a subset of CPI-refractory models (MC38, Renca, and RM1), and in all cases, mSTAR1302 improved survival compared with PBS and anti–PD-1 treatment (fig. S7).

mSTAR1302 promotes durable antitumor activity that is dependent on Vβ13 CD8$^+$T cells

To further investigate the mechanism of action of mSTAR1302, more detailed assessments were performed in the EMT6 mouse model. In this model, mSTAR1302 induced potent tumor regression compared with control molecules, demonstrating the requirement for both anti-Vβ Fab and IL-2 arms of mSTAR1302 (Fig. 4A). Compared with mice receiving PBS, mice receiving mSTAR1302 showed a marked accumulation of both CD8$^+$ T cells and granzyme B$^+$ cells in tumors as determined by immunohistochemistry staining (Fig. 4B). Flow cytometry phenotyping of isolated EMT6 TILs also highlighted mSTAR1302 dose-related increases in the frequencies of total CD8$^+$ T cells, Vβ13 CD8$^+$ T cells, and granzyme B$^+$ CD8$^+$ T cells in addition to an increase in the CD8:T_{reg} ratio (Fig. 4C). No treatment-related changes in natural killer or B cell frequencies in EMT6 tumors were observed (fig. S8A). Treatment with mSTAR1302 also increased total CD4$^+$ T cells, Vβ13 CD4$^+$ T cells, and the CD4:T_{reg} ratio, without altering T_{regs} at doses up to 1 mg/kg (fig. S8B). Furthermore, TILs isolated from IL-2 control molecule–treated mice at doses of 1 mg/kg did not show increases in total CD8$^+$ T cells, Vβ13 CD8$^+$ T cells, or granzyme B$^+$ CD8$^+$ T cells (fig. S8C), in line with the lack of tumor growth inhibition with the IL-2 control molecule in the EMT6 breast cancer model.

We found that selective depletion of Vβ13 T cells before treatment completely abrogated the antitumor activity of mSTAR1302 in the EMT6 model (Fig. 4D), confirming the importance of the de novo expansion of Vβ13 T cells. Similarly, depletion of either CD8$^+$ T cells or, to a lesser extent, CD4$^+$ T cells also resulted in a loss of mSTAR1302 antitumor activity. To investigate whether the accumulation of Vβ13 T cells in tumors also promoted long-term protective immunity, mSTAR1302-cured EMT6 mice were rechallenged 100 days after initial challenge. In all cured EMT6 mice, no tumor regrowth with EMT6 rechallenge was observed through 28 days without further mSTAR1302 treatment (Fig. 4E). In contrast, cured EMT6 mice did not reject a simultaneous de novo challenge with CT26 tumors in the opposite flank. These data suggest that mSTAR1302 promotes T cell–mediated immunity and long-term protection that is tumor specific. Moreover, the observed protective immunity appeared to be CD8$^+$ T cell dependent because depletion of CD8$^+$ T cells before tumor rechallenge resulted in EMT6 tumor growth (Fig. 4E).

mSTAR1302 induces the expansion of Vβ13 effector memory TILs with a distinct gene signature

To better understand the immune mechanisms that promote tumor clearance by expanded Vβ13 T cells, we performed a comprehensive, unbiased analysis of the EMT6 TIL transcriptome at the singe-cell level. CD4$^+$ and CD8$^+$ gene expression (fig. S9A) was weighted to assist for UMAP (Uniform Manifold Approximation and Projection) Seurat clustering and cell type annotations. As illustrated in the UMAP plot (Fig. 5A), compared with TILs from PBS-treated EMT6 mice, mSTAR1302 treatment remodeled the TIL compartment with increases in CD8$^+$ effector memory T cells (T_{EM}), CD8$^+$ naïve T cells (T_N), CD8$^+$ effector T cells (T_{EFF}), and CD4$^+$ T helper (T_H) cells. In contrast, reductions in T_{regs} and CD8$^+$ exhausted T cells were apparent after mSTAR1302 treatment. Of note, most Vβ13 T cells [inferred here through expression of *Trbv13-2* and *Trbv13-3* transcripts (fig. S9B)] mapped to the CD8$^+$ T_{EM} cluster (fig. S9C), and quantification of cell numbers further highlighted the remodeling of TILs in mSTAR1302-treated mice (Fig. 5B). Consistent with flow cytometry data, single-cell RNA sequencing (scRNA-seq) data showed increased CD8:T_{reg} ratios, CD8:CD4$^+$ T cell ratios, and nonexhausted to exhausted CD8$^+$ T cell ratios in mice treated with mSTAR1302 compared with PBS (Fig. 5C).

By comparing Vβ13 T cell subsets from mSTAR1302-treated mice versus T cells from PBS-treated mice, we identified the largest number of differentially expressed genes (DEGs) in CD8$^+$ T_{EM} cells, followed by CD8$^+$ exhausted_1, CD4$^+$ T_H, T_{reg}, and CD8$^+$ T_{EFF} clusters (Fig. 5D). Volcano plots show individual DEGs from these Vβ13 T cells with recurring genes labeled (fig. S10). Analysis of genes consistently differentially expressed across Vβ13 CD4$^+$ and CD8$^+$ T cell subsets identified a distinct gene signature (excluding ribosomal genes) specific for mSTAR1302 treatment, as illustrated in the heatmap shown in Fig. 5E (see data file S1 for full differential gene expression details). This gene signature, most pronounced in the CD8$^+$ T_{EM} cells, was characterized by genes belonging to three distinct functional groups, including (i) an up-regulation of T cell effector, memory, and cytotoxic genes, principally *Plac8*, *Il2ra*, *Ctla2a*, *Ly6c1/2*, *Gzma*, and *Gzmb*; (ii) down-regulation of genes associated with T cell exhaustion, such as *Tox*, *Nr4a1*, *Zeb2*, and *Rgs16* (*21*–*23*); and (iii) down-regulation of repressors of TCR signaling, including *Zfp36*, *Zfp36l1* (*24*), *Cd6*, and *Klf4* (*25*, *26*) (Fig. 5F). The expression of several checkpoint genes, such as *Pdcd1*, was also down-regulated in Vβ13 TILs after mSTAR1302 treatment. To investigate the specificity of the 53-gene signature identified in TILs from mice treated with mSTAR1302, we compared these genes from our study with published scRNA-seq data for IL-2, anti–PD-1 (*16*), and anti–PD-1–IL-2 mutein (IL-2v) treatments (*27*) in comparable murine syngeneic models and in similar CD8$^+$ T cell subsets. Heatmaps for this 53-gene signature across these studies illustrate the distinct nature of the mSTAR1302-induced gene expression (fig. S11A). In a gene overlap analysis restricted to those genes differentially expressed ($P < 0.01$), only 2 of the 53 genes are regulated in the same direction with IL-2 and 3 genes with anti–PD-1 treatment. The largest overlap (21 genes out of 53) was observed when comparing to genes regulated in CD8 "better effector" T cells in tumor-bearing mice treated with an anti–PD-1–IL-2v bifunctional molecule (fig. S11B). Although a very small decrease for one of the TCR repressor genes (*Zfp36l1*) was seen in TILs isolated from tumor-bearing mice treated with the anti–PD-1–IL-2v molecule, in general, the magnitude of decrease in TCR signaling repressor genes after mSTAR1302 treatment was not observed in the other published data sets (fig. S11C). Together, these transcriptomic data suggest that mSTAR1302 treatment induces a distinct shift in the pattern of gene expression in Vβ13 TILs that promotes the acquisition of highly active T_{EM} and T_{EFF} cell phenotypes that could be protected from exhaustion and sensitized for TCR signaling.

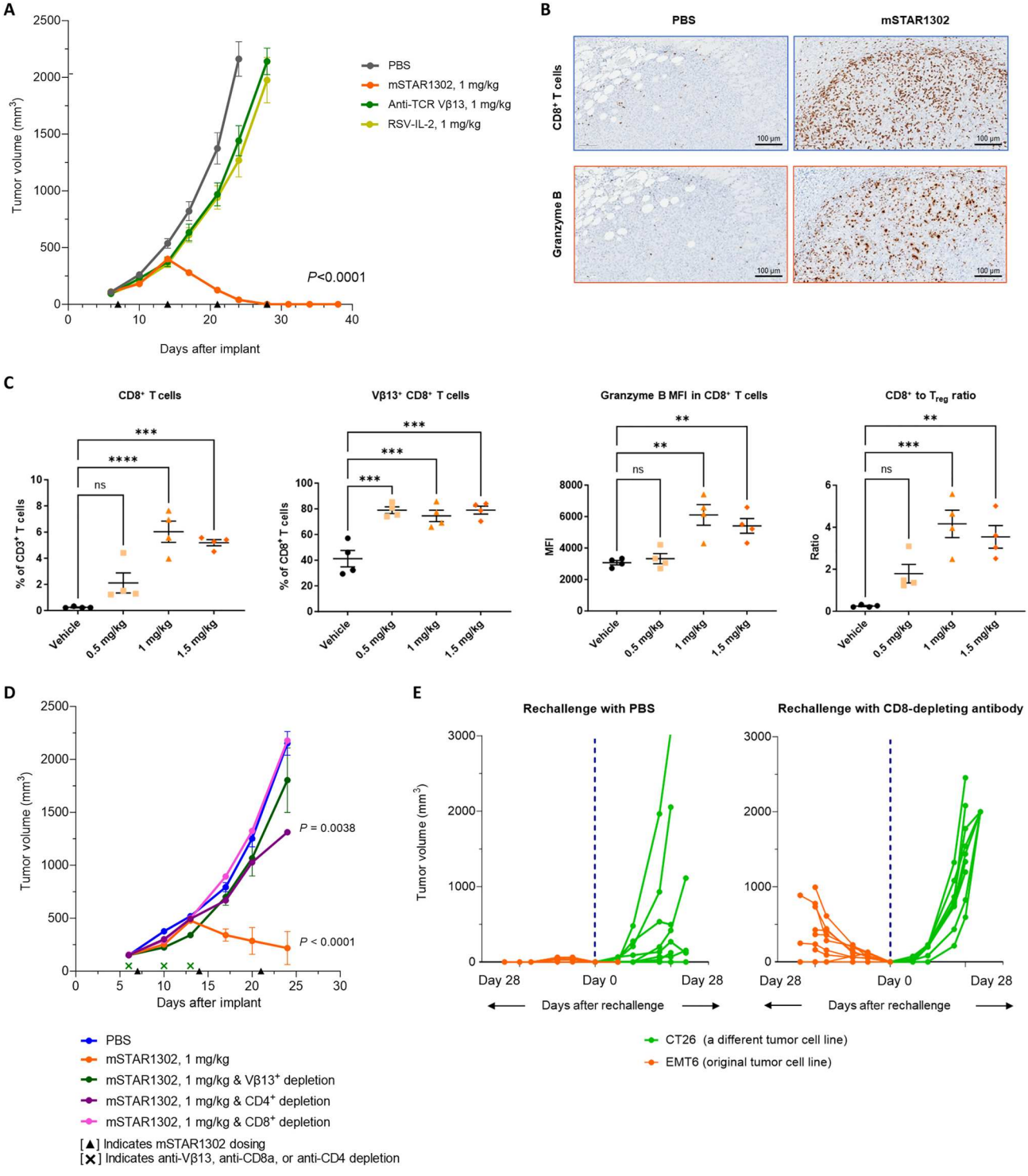

Fig. 4. mSTAR1302 induces tumor regression and protection from rechallenge in the EMT6 breast carcinoma model that is dependent on Vβ13 T cells. (**A**) Antitumor activity of four treatments of mSTAR1302 (1 mg/kg once weekly) in EMT6 mice compared with control molecules (n = 8, data are presented as mean ± SEM, significance was measured by one-way ANOVA with Brown-Forsythe and Welch tests, P < 0.0001). (**B**) Immunohistochemical staining of EMT6 tumors for CD8$^+$ T cells and granzyme B expression and (**C**) immunophenotyping of TILs isolated from EMT6 mice on day 14 after tumor implant. n = 4; data are presented as mean ± SEM; significance was measured by one-way ANOVA with Dunnett's multiple comparisons test; ****P < 0.0001, ***P < 0.001, **P < 0.01, ns = not significant. MFI, mean fluorescence intensity. (**D**) Antitumor activity of mSTAR1302 in EMT6 mice with and without depleting anti-Vβ13, anti-CD8a (6 of 10 mice died due to immunogenicity from depletion antibody treatment), or anti-CD4 (n = 10, data are presented as mean ± SEM, significance was measured by one-way ANOVA with Brown-Forsythe and Welch tests, P < 0.0001). (**E**) Cured EMT6 mice were rechallenged with EMT6 (orange curves) and CT26 (green curves) tumor cells in the absence of further treatment with mSTAR1302 and monitored for 28 days (left). n = 9. The experiment in (E) was repeated in mice that were depleted of CD8$^+$ T cells (right).

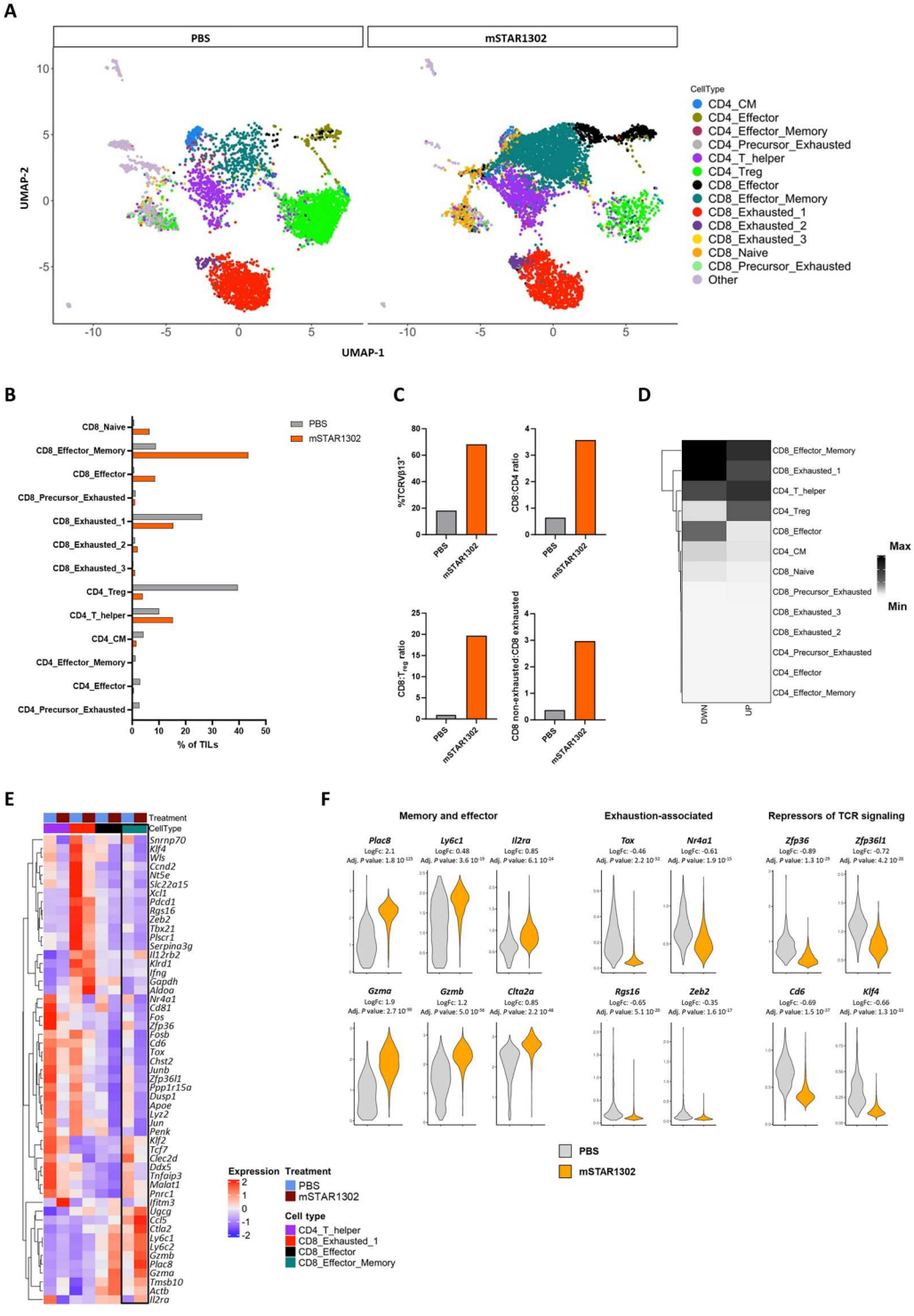

Fig. 5. mSTAR1302 induces a distinct gene signature in CD4$^+$ and CD8$^+$ TILs from the EMT6 breast carcinoma model, as measured by scRNA-seq. (**A**) UMAP of 11,685 single CD4$^+$ or CD8$^+$ TILs isolated from EMT6 mice on day 14 after tumor implant after a single dose of mSTAR1302 (right) or PBS (left) from $n = 5$ mice pooled per group. (**B**) Quantification (%) of cell subsets in EMT6 TILs from mice treated with PBS or mSTAR1302 and (**C**) quantification of Vβ13 T cells and indicated T cell ratios. (**D**) Heatmap of the number of differentially expressed genes (DEGs) in TILs when comparing Vβ13$^+$ subsets from mSTAR1302 versus all T cell subsets in PBS-treated mice. (**E**) Heatmap of DEGs from the same samples as (D) constituting the gene signature in response to mSTAR1302 treatment compared with PBS across indicated T cell subsets. Expression values scaled for each gene. (**F**) Violin plots of selected DEGs in the same samples as (D) comparing imputed gene expression for PBS- and mSTAR1302-treated groups in CD8$^+$ T_{EM} cells.

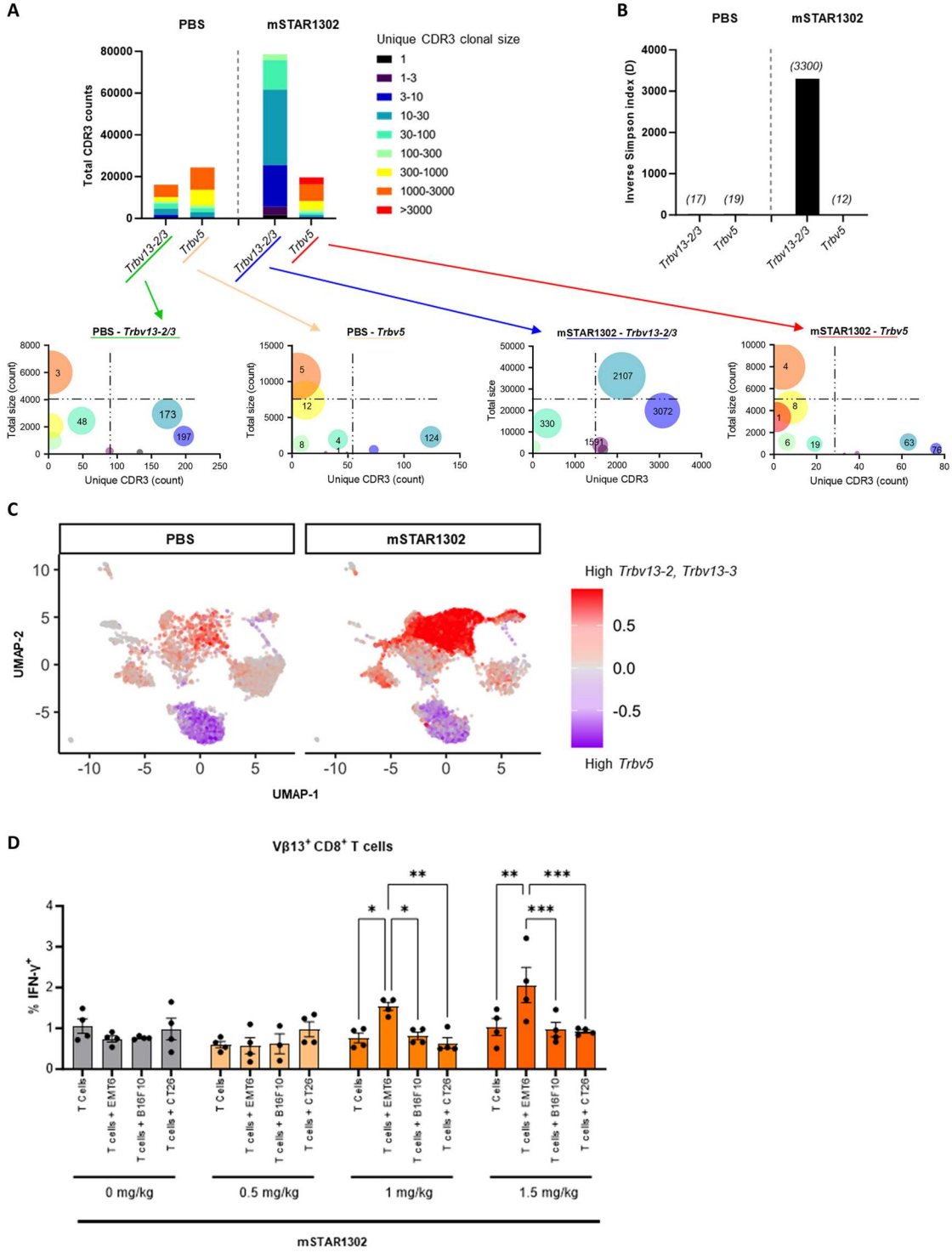

Fig. 6. mSTAR1302 increases TCR diversity in CD4$^+$ and CD8$^+$ Vβ TIL subsets from EMT6 breast carcinoma model. (**A**) The top plot shows clonal CDR3 counts for targeted Vβ13 T cells (expressing *Trbv13-2/3* transcripts) and nontargeted Vβ5 T cells (expressing *Trbv5* transcripts) from EMT6 TILs. $n = 4$ mice pooled per group. The lower bubble plots show total CDR3 counts and unique CDR3 sequences within the *Trbv13-2/3* and *Trbv5* genes in PBS- and mSTAR1302-treated groups (color indicates clonal size; size indicates percentage of total CDR3 counts within respective *Trbv* genes; text within each bubble indicates number of unique CDR3 sequences). (**B**) TCR diversity of TILs within *Trbv13-2/3* or *Trbv5* as in (A), calculated as inverse Simpson's diversity index. (**C**) scRNA-seq UMAP indicating *Trvb13-2/3* (red) and *Trbv5* (purple) T cells in TILs from PBS- (left) and mSTAR1302- (right) treated mice. (**D**) Ex vivo tumor antigen recall assay within Vβ13 CD8$^+$ T cell splenocytes isolated from EMT6 tumor–bearing mice that were treated weekly with 0, 0.5, 1, or 1.5 mg/kg mSTAR1302 and cocultured with EMT6 cell lysates for 16 hours to elicit T cell responses. B16F10 and CT26 tumor cell lysates were used as negative controls. Responses were quantified by IFN-γ intracellular flow cytometry staining. $n = 4$ mice per group; significance was measured by two-way ANOVA with Bonferroni's multiple comparisons test; ***$P < 0.001$, **$P < 0.01$, *$P < 0.05$; data are presented as mean ± SEM.

mSTAR1302 expands the TCR repertoire in TILs

To further understand the impact of mSTAR1302 treatment on TCR repertoire usage in TILs, TCR sequencing of treated EMT6 TILs was performed. As shown in Fig. 6A and fig. S12A, TILs isolated from PBS-treated EMT6 mice generally exhibited oligoclonal TCRs, with a few dominant T cell clones sharing the same CDR3 sequence and most clones expressed within the Vβ5 and Vβ13 subsets. In contrast, TILs isolated from mSTAR1302-treated mice showed an increase in the number of unique CDR3s with smaller clonal sizes (indicating increased diversity of CDR3 repertoires) in the expanded Vβ13 TIL population. In contrast, the non-Vβ13 T cells (e.g., Vβ5) that are not targeted by mSTAR1302 maintained low TCR diversity with substantial single CDR3 clonal expansion. The increase in diversity within Vβ13 T cells was also apparent when plotting total CDR3 size versus unique CDR3 (Fig. 6A), where counts are shown in a "bubble" plot for both Vβ13 and Vβ5 TILs from mice treated with mSTAR1302 or PBS. TCR diversity was also quantified using an inverse Simpson index that further reflects the increased repertoire diversity associated with mSTAR1302 (Fig. 6B). Although most Vβ13 T cells expanded by mSTAR1302 were T_{EM} cells, nontargeted Vβ5 cells were predominantly restricted to the $CD8^+$ exhausted T cell cluster (Fig. 6C). To further investigate the functional relevance of the observed increase in TIL CDR3 TCR repertoire diversity, we performed an ex vivo antigen recall assay on T cells isolated from spleens of EMT6 tumor–bearing mice treated with different doses of mSTAR1302. Using naïve splenocytes as antigen-presenting cells, splenocytes from mSTAR1302-treated EMT6 mice were cocultured with EMT6 tumor cell lysates (B16F10 and CT26 tumor cell lysates were used as negative controls) to explore the tumor specificity of T cell responses using intracellular IFN-γ staining. Using this ex vivo "recall" assay, robust T cell responses were observed in Vβ13 $CD8^+$ T cells from mSTAR1302-treated animals challenged with EMT6 tumor cell lysates, whereas no T cell activation was observed in response to challenge with B16F10 or CT26 tumor cell lysates (Fig. 6D). Consistent with the data from EMT6 TILs, TCR diversity as determined by clonal sizes and the inverse Simpson index was also increased substantially in Vβ13 T cells after mSTAR1302 treatment of mice bearing either MC38 (fig. S12B) or CT26 tumors (fig. S12C). This increase was not observed for mice treated with the IL-2 control molecule. Finally, to further confirm the repertoire of tumor antigen-specific T cell responses within Vβ13 T cells, we stained TILs isolated from mSTAR1302-treated CT26 tumors with major histocompatibility complex (MHC) class I tetramers to the tumor rejection antigen AH1/gp70 [a murine leukemia virus (MuLV) envelope protein] (*28*). Higher frequencies of AH1/gp70 $tetramer^+$ $CD8^+$ T cells were present in Vβ13 $CD8^+$ T cells from mSTAR1302-treated mice compared with PBS-treated mice, with minimal frequencies of AH1/gp70-specific T cells present in non-Vβ13 T cells (fig. S12D). Numerous antigen-specific TCR CDR3 sequences from AH1/gp70-specific murine T cells have been reported previously (*28*, *29*), and by matching these known sequences to CDR3 sequences within the Vβ13 T cell repertoire from mSTAR1302-treated mice, we identified 20 known AH1/gp70 CDR3 sequences that were not observed in Vβ13T cells from PBS-treated mice (table S5). These data also support the possibility that the observed increases in CDR3 repertoire diversity within expanded Vβ13 T cells from mSTAR1302-treated mice represent an expansion of the repertoire to dominant tumor antigens.

STAR0602 selectively expands target Vβ6 T cells in nonhuman primates

To support the characterization of STAR0602 in nonhuman primates, cross-reactivity was confirmed by measuring the binding of STAR0602 to purified cynomolgus Vβ6 TCR and IL-2R proteins. STAR0602 bound to cynomolgus Vβ6-2 (4.9 nM), IL-2Rα (CD25, 48 nM), and IL-2Rβγ (3.3 nM) with high affinity that was similar to binding with human Vβ6 TCR and IL-2R proteins (table S1). The pharmacokinetics of a single intravenous dose of STAR0602 were characterized by rapid nonlinear clearance over the dose range tested (Fig. 7A and table S6). Despite this rapid clearance, sustained expansion of target Vβ6/Vβ10 $CD8^+$ T cells (two- to threefold increase over baseline) and, to a lesser extent, $CD4^+$ T cells was observed in the blood of STAR0602-treated monkeys, peaking at day 6 after infusion (Fig. 7B). Limited to no expansion of $FoxP3^+$ T_{regs} was observed over a similar timeframe to the expansion of $CD8^+$ and conventional $CD4^+$ T cells. This Vβ6/Vβ10 lymphocytosis was more profound in the $CD8^+$ T cell compartment and was preceded by transient and reversible peripheral lymphopenia due to tissue margination of activated T cells immediately after dosing. The magnitude of Vβ6/Vβ10 T cell expansion observed in the blood of monkeys was consistent with the magnitute of Vβ13 T cell expansion associated with antitumor activity of mSTAR1302 in tumor-bearing mice. To confirm engagement of the IL-2R pathway by STAR0602, pSTAT5 and soluble CD25 (sCD25) were assessed in PBMCs and sera from treated monkeys. As expected, pSTAT5 increased immediately after dosing with STAR0602, indicating activation of the IL-2R pathway, with sCD25 concentrations peaking at 48 hours after infusion (Fig. 7C). Finally, only moderate cytokine release was observed in the blood of monkeys after infusion of STAR0602 (Fig. 7D). Cytokine concentrations generally peaked around 48 hours after STAR0602, with peak concentrations of 0.4 ng/ml for IFN-γ, 0.7 ng/ml for IL-6, and 1.0 ng/ml for tumor necrosis factor–α (TNF-α). Peak concentrations were generally 50 to 90% lower than in published reports of cytokine release in monkeys administered a single intravenous dose of bispecific anti-CD3 antibodies (*30*, *31*). Regarding the potential for IL-2–related toxicities, we also observed minimal increase in peripheral IL-5 concentrations and eosinophils (*28*, *29*), markers associated previously with IL-2 toxicity (*32*), in monkeys dosed with 1 mg/kg STAR0602 (Fig. 7E). Similarly, no discernible changes in serum concentrations of liver enzyme markers of IL-2–induced hepatic injury were observed across 0.5 to 1.5 mg/kg STAR0602 doses (fig. S13), and no serious toxicities, body weight loss, or deaths were observed after dosing of intravenous STAR0602 in cynomolgus monkeys.

STAR0602 promotes the ex vivo expansion of human TILs that kill patient-derived tumor organoids and expands antigen-specific T cells

As shown in representative images from an ex vivo human tumor organoid culture derived from a patient with rectal cancer, STAR0602 promoted the expansion of human TILs (blue), effectively reduced tumor organoid size (red), and increased the proportion of dead tumor cells (green) (Fig. 8A). The frequency of Vβ6/Vβ10 T cells varied among the four organoid models tested, ranging from 6 to 28% of autologous TILs (Fig. 8B), with three of these models being refractory to pembrolizumab (Fig. 8C). STAR0602 effectively reduced organoid size in three of four models, one of which was sensitive to pembrolizumab and two that were refractory to

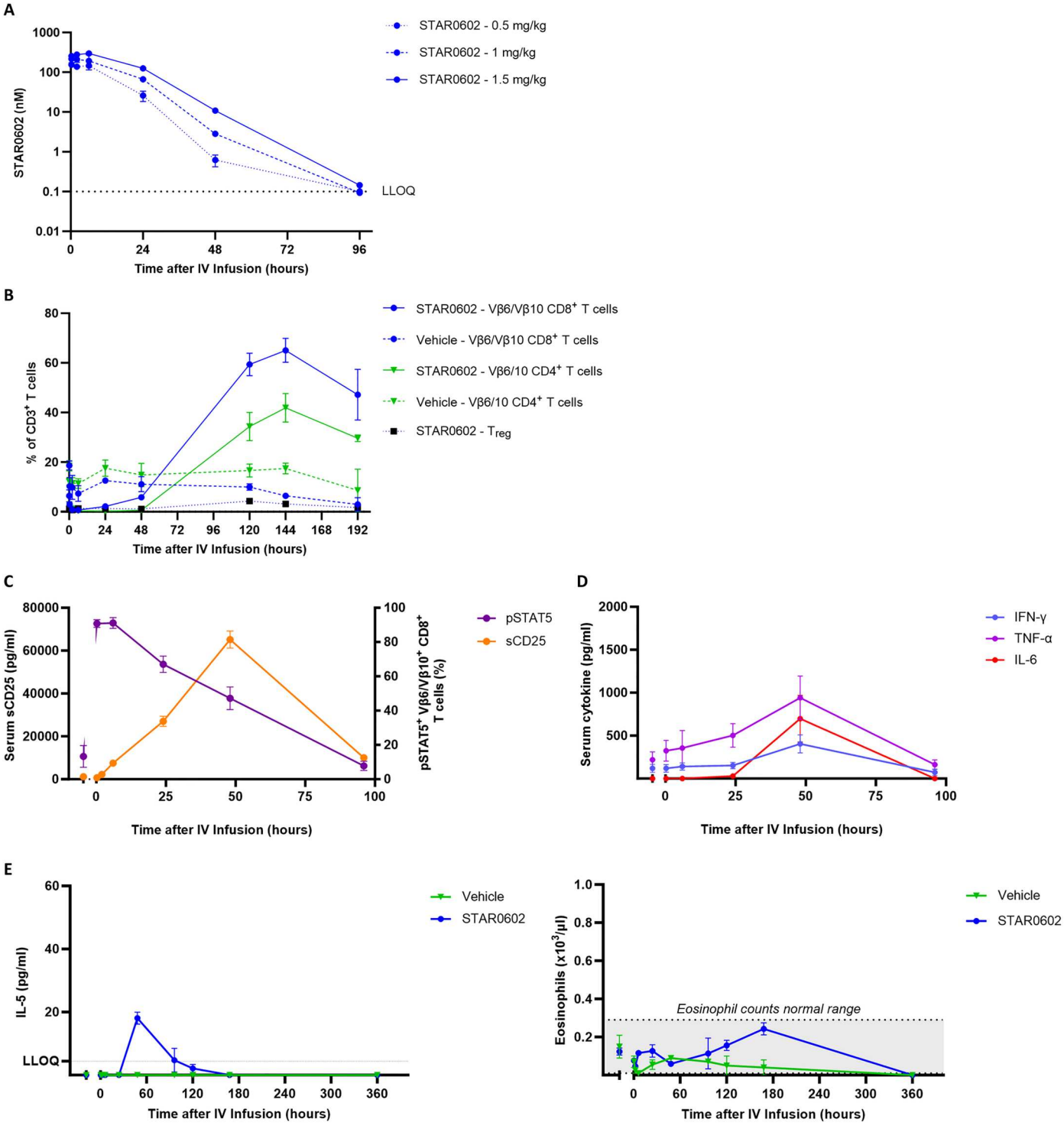

Fig. 7. STAR0602 selectively expands target Vβ6 T cells in nonhuman primates with moderate cytokine release. (**A**) STAR0602 serum concentrations after single intravenous (IV) dosing in cynomolgus monkeys. LLOQ, lower limit of quantification. $n = 2$ (0.5 and 1.5 mg/kg) and $n = 3$ (1 mg/kg); data are presented as mean ± SEM. (**B**) $CD8^+$ and $CD4^+$ Vβ6/Vβ10 T cell and T_{reg} frequency in blood after single STAR0602 1 mg/kg intravenous dose; $n = 3$, data are presented as mean ± SEM. (**C**) Serum concentrations of soluble CD25 and frequencies of $pSTAT5^+$ $CD8^+$ T cells after a single STAR0602 0.5 mg/kg intravenous dose; $n = 6$, data are presented as mean ± SEM. (**D**) Serum concentrations of indicated cytokines after a single STAR0602 0.5-mg/kg intravenous dose; $n = 6$; data are presented as mean ± SEM. (**E**) IL-5 concentrations and eosinophil counts measured before and after a single STAR0602 1 mg/kg intravenous dose. The gray shaded region indicates the normal range of eosinophil counts; $n = 3$; data are presented as mean ± SEM.

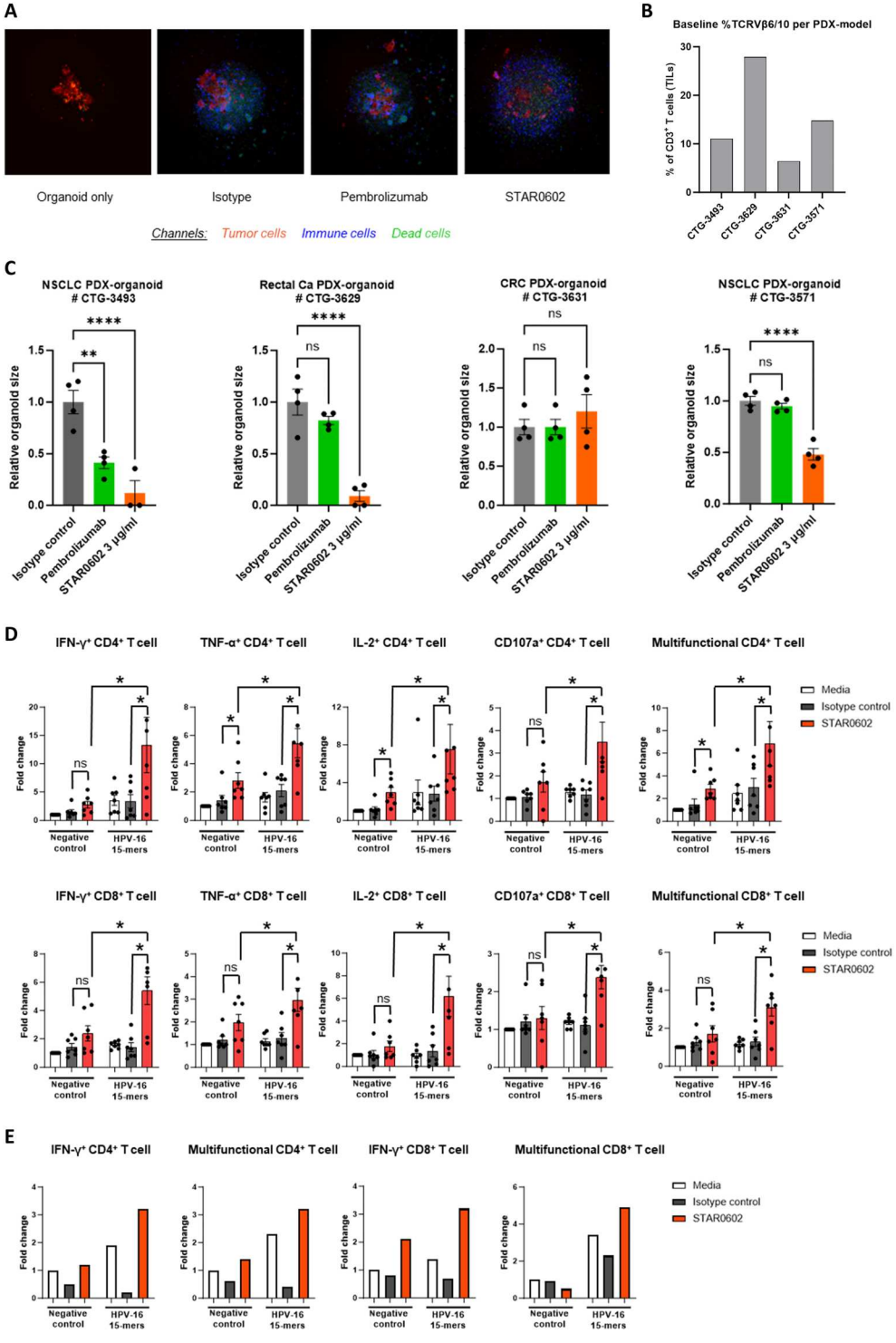

Fig. 8. STAR0602 shows antitumor activity in an ex vivo human tumor organoid model and expands antigen-specific T cells. (**A**) High-content image of a human rectal cancer organoid with autologous TILs incubated with STAR0602 (3 μg/ml), anti–PD-1 (pembrolizumab, 10 μg/ml), or isotype control (3 μg/ml) for 5 days. Immune (blue), tumor (red), and dead (green) cells are shown. (**B**) Baseline Vβ6/Vβ10 T cell frequency in TILs from the four organoids. (**C**) Summary of cancer organoid killing across four models ($n = 4$; data are presented as mean ± SEM of technical quadruplets; significance was measured by one-way ANOVA with Dunnett's multiple comparisons test; $^{****}P < 0.0001$, $^{**}P < 0.01$). (**D**) Ex vivo activation of HPV-16–specific T cells by STAR0602 in PBMCs from healthy donors ($n = 7$, data are presented as mean ± SEM, $^{*}P < 0.05$). Significance was measured by the Wilcoxon signed rank test. (**E**) Ex vivo activation of HPV-16–specific T cells by STAR0602 in PBMCs from a patient with cervical cancer. In (D) and (E), PBMCs were treated for 1 hour with 1 nM STAR0602, the isotype control, or media and then stimulated with HPV-16 peptides or a negative control and stained for intracellular expression of IFN-γ, TNF-α, IL-2, and CD107a; multifunctional T cells were those positive for two or more among these markers tested.

pembrolizumab (Fig. 8C). Furthermore, reduction of organoid size was dependent on STAR0602 concentration and was not observed with the IL-2 control molecule (fig. S14A).

Finally, we investigated the ability of STAR0602 to expand human antigen-specific T cells in vitro. As shown in Fig. 8D, STAR0602 expanded human papillomavirus-16 (HPV-16)–specific $CD4^+$ and $CD8^+$ T cells when stimulated with HPV-16 peptides, as evidenced by enhanced numbers of T cells producing IFN-γ, TNF-α, and IL-2, as well as T cells positive for CD107a, compared with the isotype control (Fig. 8D). This expansion was not observed with the soluble anti-Vβ6/Vβ10 antibody control (fig. S14B). STAR0602 expanded both multifunctional $CD4^+$ and $CD8^+$ HPV-16–specific T cells, defined as T cells positive for two or more of the functional markers examined. Similar findings were observed in PBMCs from a patient with cervical cancer. Here, STAR0602 increased the number of HPV-16 $CD4^+$ and $CD8^+$ T cells producing IFN-γ and multifunctional HPV-16 $CD4^+$ and $CD8^+$ T cells (Fig. 8E).

DISCUSSION

Antibody targeting of the TCR is an effective strategy to activate T cells, which can be enhanced by engaging costimulatory signals (*33*). Recent in vitro studies of plate-coated anti-Vβ TCR antibodies highlight their utility in driving selective activation and expansion of human T cells expressing different germline-encoded Vβ TCR chains (*18*). Here, we extend those studies by testing a therapeutic T cell activator (STAR0602) that achieves activation and expansion of germline Vβ T cell subsets in solution and promotes potent antitumor activity.

To support the development of a pan-tumor T cell immunotherapy, we designed STAR0602 to target Vβ6 T cell subsets, because based on our assessment of Vβ6 TCR expression in TILs from patient tumors and previously published data (*11*), Vβ6 T cells are enriched in TILs relative to other Vβ subsets and are present in all cancers. By gradually expanding this smaller subset of T cells rather than activating all T cells as with agonist anti-CD3 antibodies, we also hypothesized that adverse events associated with T cell activation (e.g., cytokine release) might be reduced.

Our studies demonstrate that the STAR0602 molecule, comprising monovalent binding to Vβ6 and Vβ10 TCRs, and IL-2 binding to IL-2Rs, selectively activates and expands human Vβ6/Vβ10 T cells wherein both arms are necessary for T cell activation. Prior studies of TCR-activating antibodies suggest a requirement for TCR cross-linking with multivalent antibodies or presentation on a solid phase (*34*). However, we show here that, in solution, a monovalent TCR binding Fab fused to a cytokine ligand can robustly stimulate both TCR and IL-2R signaling and recapitulate the T cell characteristics induced by plate-coated anti-Vβ6 antibodies. The precise mode of TCR engagement by STAR0602 remains to be defined but may involve clustering of IL-2Rs with Vβ6 TCRs on cellular lipid rafts or, alternatively, involve an allosteric mode of TCR activation (*35*). STAR0602 also shows avidity-enhanced binding of the IL-2 moiety in cis in an anti-Vβ TCR Fab-dependent manner. Together with the approximately 100-fold reduction in IL-2R signaling potency of STAR0602 observed in the pSTAT5 bioactivity assay, these observations suggest restricted and conditional activity of the IL-2 moiety of STAR0602 that may limit the potential for idiosyncratic on-target/off-tissue IL-2 toxicity (*19*, *32*) and may explain why STAR0602 is well tolerated in mice and nonhuman primates at doses exceeding the maximum tolerated dose of rhIL-2.

The tumor regression observed in mice treated with the murine surrogate molecule mSTAR1302 compared with PBS was durable, with cures maintained through >100 days and long-term protection from tumor rechallenge that was dependent on $CD8^+$ T cells. It has been suggested that the responsiveness of syngeneic mouse tumor models to immunotherapy might be affected by either the mouse strain used or environmental factors, such as mouse housing conditions, that might modulate the murine microbiome (*36*, *37*). However, we observed consistent antitumor activity with mSTAR1302 across six different tumor models and in several models that were performed at different sites and with mice from different vendors.

The infiltration of activated $CD8^+$ granzyme B^+ Vβ13 T cells into the usually immune-excluded EMT6 tumors (*38*), and the loss of antitumor activity with depletion of these cells, implicates the de novo expansion of memory Vβ13 T cells in the antitumor activity of mSTAR1302. The analysis of Seurat clusters from EMT6 TILs further highlights the mSTAR1302-induced expansion of Vβ13 T cells in murine tumors, with profound remodeling of the TIL compartment characterized by a substantial increase in Vβ13 $CD8^+$ T_{EM} cells and a decrease in $FoxP3^+$ T_{regs}. The predominance of this T_{EM} T cell phenotype in murine TILs stands in contrast to the phenotype observed in STAR0602-stimulated human T cells in vitro, where STAR0602 induced the selective expansion of Vβ6/Vβ10 T cells that acquired a homogenous $CD95^+$ $CCR7^+$ $CD45RA^-$ T_{CM} phenotype that was considered atypical because of the coexpression of cytotoxic and effector molecules, such as IFN-γ, granzyme B, and CD25. However, these differences in T cell memory states across experiments are likely due to the influence of the TME in in vivo studies compared with in vitro studies and differences in the timing of sampling between in vivo and in vitro assays. It is also notable that, although small in numbers, T_{CM} and other precursor T cell subsets were observed in mSTAR1302-treated mice, whereas they were almost absent in PBS-treated mice. A deeper analysis of the transcriptome of these expanded Vβ13 T cells revealed a gene signature characterized by up-regulation of *Plac8*, along with up-regulation of *Ctla2a*, *Il2ra*, and the T cell memory/effector gene *Ly6c1* across numerous T cell subtypes. This signature suggests reprogramming to a mixed effector/memory phenotype reminiscent of the phenotype induced in human T cells by STAR0602.

The role of *Plac8* in T cell function is poorly understood but appears to be critical for the development of effective $CD8^+$ memory T cell responses to viral pathogens and the control of T_H1 $CD4^+$ T cell responses (*39*). Recently, a similar gene signature of *Plac8*, *Ctla2a*, *Ly6c2*, and *Klrd1* was also associated with restoration of $CD4^+$ effector T cell responses in a murine model of chronic infection and T cell exhaustion (*40*), suggesting relevance of this signature in promoting productive effector T cell responses. In contrast, the expression of genes associated with stem-like $CD8^+$ T cells, including *Tcf7* and *Pdcd1* (*27*, *41*), and transcriptional regulators of T cell exhaustion, such as *Tox*, *Rgs16*, and *Nr4a1* (*21*–*23*), was decreased in the expanded Vβ13 $CD8^+$ T_{EM} population.

Reduced expression of several TCR regulatory genes, including the RNA binding repressor proteins *Zfp36* and *Zfp36l1* (*24*, *42*) and other TCR signaling repressors (e.g., *Cd6* and *Klf4*) that control the tempo of T cell activation (*25*, *26*), suggests that derepression of TCR signaling by mSTAR1302 might also be a mechanism

through which expanded Vβ TILs achieve higher effector potentials. The regulation of these TCR signaling repressor genes appears to be a distinct feature of the action of mSTAR1302, because few to no changes in these genes were found in a comparative analysis of published transcriptomic data from analogous $CD8^+$ T cell subsets in mouse models treated with other T cell–directed immunotherapies, including anti–PD-1, IL-2 (*16*), or a bifunctional anti–PD-1–IL-2 mutein molecule (*27*).

Together with the increases in CDR3 repertoire diversity, these data suggest that mSTAR1302 antitumor activity is mediated by the expansion of a clonally diverse population of Vβ13 $CD8^+$ effector memory T cells and $CD4^+$ T_H1 memory T cells. This apparent clonal "revival" within expanded Vβ13 TILs suggests either expansion of low-abundance tumor-resident T cells or clonal replacement through expansion and infiltration of Vβ13 T cell precursors from other T cell niches. In contrast, response to anti–PD-1 therapy in humans is associated with limited expansion of mainly precursor exhausted T cells (T_{EXP}) with modest clonal revival or replacement associated with clinical response (*43*, *44*), suggesting that the expansion of clonally enriched Vβ T_{EM} TILs might support the potential for improved antitumor activity of STAR0602 compared with CPI therapy.

In tumor-bearing mice, the two- to threefold expansion of Vβ13 T cells in blood and tumor tissue was shown to be a critical determinant of the antitumor activity of mSTAR1302. Thus, the selective expansion of Vβ6/Vβ10 T cells at a similar magnitude in the blood of monkeys dosed with intravenous STAR0602 supports the potential for translation of the antitumor activity observed in mice into humans. Moreover, although translation of cytokine release profiles from monkeys to humans is relatively poor, the limited and delayed cytokine release observed in monkeys and limited expression of biomarkers of IL-2 toxicity suggests the potential for a more workable therapeutic index than observed with rhIL-2 and other T cell engagers (*31*).

Because the antitumor activity of STAR0602 is likely to be linked to expansion and remodeling of endogenous tumor antigen-specific T cell responses, the translational pharmacology of STAR0602 was assessed in ex vivo human tumor organoid models with intact (autologous) human TIL responses, rather than xenogeneic humanized mouse models. In these organoids, STAR0602 effectively expanded and converted tumor-resident, antigen-specific Vβ6/Vβ10 T cells into more productive effectors that potently killed tumor cells to a much greater extent than treatment with the anti–PD-1 antibody pembrolizumab. This effect was further extended by in vitro studies demonstrating that human HPV-16–specific T cells from both a patient with cancer and healthy donors were boosted in the presence of STAR0602.

Given the putative STAR0602 mechanism of activating and expanding endogenous, antigen-specific T cell responses, we used immunocompetent (syngeneic) tumor-bearing mouse models rather than xenogeneic models with human tumors and engrafted allogeneic human PBMCs. Although these syngeneic models are very useful, they have limitations. For example, unlike advanced tumors identified in humans, murine tumors are highly homogeneous and engrafted into mice with naive immune systems that readily respond to the undefined and highly immunogenic determinants on tumor cell lines. Moreover, the use of fully murine models necessitated testing with a murine surrogate molecule, mSTAR1302, that, although of the same design and in vitro pharmacology to STAR0602, might have subtly different in vivo properties by virtue of targeting murine Vβ13 T cells compared with human Vβ6 T cells. Although the phenotypic changes to Vβ TILs were extensively assessed, we did not explore the role of tumor-intrinsic factors, such as the impact of changes in antigen-presenting machinery, which warrant further study. Finally, whether Vβ T cells are predominantly expanded within the tumor or at other sites (e.g., tumor-draining lymph nodes or blood) and then traffic to the tumor remains to be elucidated but is likely to be an important component of the mechanism of action.

Using therapeutic antibodies to selectively expand Vβ T cell subsets and thereby modulate the germline TCR repertoire is a distinct modality of T cell activation. Although, by convention, the distinct Vβ and Vα genes are thought to be semi-randomly incorporated into TCRs (*9*), the observed usage of V genes across the human TCR repertoire is not entirely stochastic, as reflected by skewed usage of certain V genes in TILs from large cohorts of patients with cancer (*11*) and in T cell responses to various infectious pathogens (*45*). Such skewing in V gene usage likely reflects selection bias on certain CDR1 and CDR2 sequences, because of either linkage to MHC alleles (*46*) and non-MHC antigen-presenting molecules (*47*) or the direct involvement of these regions in antigen recognition (*48*). Thus, in addition to the pan-tumor approach described here, the use of anti-Vβ antibody therapeutics to modulate T cells with common V genes has broad application across different diseases, including the possibility of modulating germline-dominant antigen-specific T cell responses in cancer and infectious diseases, modulating T cell subsets expressing invariant and semi-invariant TCRs, and deploying combinations of anti-Vβ therapeutics. By incorporating different costimulatory factors into this bifunctional antibody format, further tuning of T cell responses could also be envisaged.

Because STAR0602 achieves antitumor activity through a distinct mechanism to existing immunotherapies, future studies should be considered to determine its potential for combination with CPIs, vaccines, chemotherapy, and other small-molecule targeted therapies. However, the studies of STAR0602 in vitro, in nonhuman primates, and in primary patient-derived organoids, and of mSTAR1302 in several syngeneic murine models described here, support further investigations of STAR0602 in humans. It is evident that much work needs to be performed to define optimal use of STAR0602 in humans, including dose and schedule. Therefore, a phase 1/2 first-in-human, open-label, dose escalation and expansion study of STAR0602 (NCT05592626) in patients with advanced metastatic cancer has recently commenced. Collectively, our data suggest that STAR0602 may provide a well-tolerated, off-the-shelf T cell immunotherapy with enhanced antitumor activity in cancer patients.

MATERIALS AND METHODS

Study design

The objective of this study was to develop a bispecific antibody fusion molecule that selectively targets certain TCR β chains and induces T cell activation, expansion, and antitumor activity. Using the bifunctional STAR0602 molecule comprising an antibody targeting Vβ6/10 T cells fused to human IL-2 and murine surrogate molecule (mSTAR1302) of the same design targeting Vβ13 T cells, we investigated the primary pharmacology, selectivity,

immunology, and antitumor activity across a range of in vitro and in vivo models. All constructs were produced and purified at Marengo. Human patient-derived organoid and syngeneic mouse models were used to evaluate the antitumor activity of these molecules, and scRNA-seq was performed on TILs isolated from mouse tumors treated with mSTAR1302. Finally, the in vivo pharmacology and immunology of single intravenous doses of STAR0602 were investigated in cynomolgus monkeys. All animal experiments were performed in compliance with established ethical regulations and were approved by the Institutional Animal Care and Use Committee (IACUC) at CRADL (Charles River Accelerator & Development Lab).

Statistical analysis

Primary data are presented in data file S2. Data were analyzed in GraphPad Prism 9 software. Data with two groups were analyzed by unpaired Student's *t* test or Wilcoxon match-pairs signed rank test. Data with multiple groups were analyzed by one-way analysis of variance (ANOVA) with Brown-Forsythe Welch tests, Dunnett's multiple comparisons test, or two-way ANOVA with Bonferroni's multiple comparisons test. Survival curves were analyzed by log-rank (Mantel-Cox) test. Data are shown as mean ± SEM. Significance is shown as $^{****}P < 0.0001$, $^{***}P < 0.001$, $^{**}P < 0.01$, $^{*}P < 0.05$, or ns = not significant. Outliers were not excluded for any of the analyses. Experiments repeated more than once in independent experiments with similar results and symbol representations are defined in legends. Technical replicates are indicated in legends where used. *n* represents the number of biologic replicates (animals or sample sizes).

Supplementary Materials

This PDF file includes:
Materials and Methods
Figs. S1 to S15
Tables S1 to S6
References (*49*, *50*)

Other Supplementary Material for this manuscript includes the following:
Data files S1 and S2
MDAR Reproducibility Checklist

References and Notes

1. M. A. Postow, M. K. Callahan, J. D. Wolchok, Immune checkpoint blockade in cancer therapy. *J. Clin. Oncol.* **33**, 1974–1982 (2015).
2. A. L. Garfall, M. V. Maus, W. T. Hwang, S. F. Lacey, Y. D. Mahnke, J. J. Melenhorst, Z. Zheng, D. T. Vogl, A. D. Cohen, B. M. Weiss, K. Dengel, N. D. Kerr, A. Bagg, B. L. Levine, C. H. June, E. A. Stadtmauer, Chimeric antigen receptor T cells against CD19 for multiple myeloma. *N. Engl. J. Med.* **373**, 1040–1047 (2015).
3. M. E. Goebeler, S. Knop, A. Viardot, P. Kufer, M. S. Topp, H. Einsele, R. Noppeney, G. Hess, S. Kallert, A. Mackensen, K. Rupertus, L. Kanz, M. Libicher, D. Nagorsen, G. Zugmaier, M. Klinger, A. Wolf, B. Dorsch, B. D. Quednau, M. Schmidt, J. Scheele, P. A. Baeuerle, E. Leo, R. C. Bargou, Bispecific T-Cell Engager (BiTE) antibody construct blinatumomab for the treatment of patients with relapsed/refractory non-hodgkin lymphoma: Final results from a phase I study. *J. Clin. Oncol.* **34**, 1104–1111 (2016).
4. E. K. Moon, L. C. Wang, D. V. Dolfi, C. B. Wilson, R. Ranganathan, J. Sun, V. Kapoor, J. Scholler, E. Puré, M. C. Milone, C. H. June, J. L. Riley, E. J. Wherry, S. M. Albelda, Multifactorial T-cell hypofunction that is reversible can limit the efficacy of chimeric antigen receptor-transduced human T cells in solid tumors. *Clin. Cancer Res.* **20**, 4262–4273 (2014).
5. S. L. Topalian, F. S. Hodi, J. R. Brahmer, S. N. Gettinger, D. C. Smith, D. F. McDermott, J. D. Powderly, R. D. Carvajal, J. A. Sosman, M. B. Atkins, P. D. Leming, D. R. Spigel, S. J. Antonia, L. Horn, C. G. Drake, D. M. Pardoll, L. Chen, W. H. Sharfman, R. A. Anders, J. M. Taube, T. L. McMiller, H. Xu, A. J. Korman, M. Jure-Kunkel, S. Agrawal, D. McDonald, G. D. Kollia, A. Gupta, J. M. Wigginton, M. Sznol, Safety, activity, and immune correlates of anti-PD-1 antibody in cancer. *N. Engl. J. Med.* **366**, 2443–2454 (2012).
6. T. E. Keenan, K. P. Burke, E. M. Van Allen, Genomic correlates of response to immune checkpoint blockade. *Nat. Med.* **25**, 389–402 (2019).
7. J. M. Taube, A. Klein, J. R. Brahmer, H. Xu, X. Pan, J. H. Kim, L. Chen, D. M. Pardoll, S. L. Topalian, R. A. Anders, Association of PD-1, PD-1 ligands, and other features of the tumor immune microenvironment with response to anti-PD-1 therapy. *Clin. Cancer Res.* **20**, 5064–5074 (2014).
8. M. Yarchoan, A. Hopkins, E. M. Jaffee, Tumor mutational burden and response rate to PD-1 inhibition. *N. Engl. J. Med.* **377**, 2500–2501 (2017).
9. J. E. Smith-Garvin, G. A. Koretzky, M. S. Jordan, T cell activation. *Annu. Rev. Immunol.* **27**, 591–619 (2009).
10. J. P. Snook, C. Kim, M. A. Williams, TCR signal strength controls the differentiation of CD4(+) effector and memory T cells. *Sci. Immunol.* **3**, (2018).
11. B. Li, T. Li, J. C. Pignon, B. Wang, J. Wang, S. A. Shukla, R. Dou, Q. Chen, F. S. Hodi, T. K. Choueiri, C. Wu, N. Hacohen, S. Signoretti, J. S. Liu, X. S. Liu, Landscape of tumor-infiltrating T cell repertoire of human cancers. *Nat. Genet.* **48**, 725–732 (2016).
12. A. C. Hayday, P. Vantourout, The innate biologies of adaptive antigen receptors. *Annu. Rev. Immunol.* **38**, 487–510 (2020).
13. G. Hedlund, M. Dohlsten, C. Petersson, T. Kalland, Superantigen-based tumor therapy: In vivo activation of cytotoxic T cells. *Cancer Immunol. Immunother.* **36**, 89–93 (1993).
14. G. Forsberg, L. Ohlsson, T. Brodin, P. Björk, P. A. Lando, D. Shaw, P. L. Stern, M. Dohlsten, Therapy of human non-small-cell lung carcinoma using antibody targeting of a modified superantigen. *Br. J. Cancer* **85**, 129–136 (2001).
15. D. M. Shaw, N. B. Connolly, P. M. Patel, S. Kilany, G. Hedlund, O. Nordle, G. Forsberg, J. Zweit, P. L. Stern, R. E. Hawkins, A phase II study of a 5T4 oncofoetal antigen tumour-targeted superantigen (ABR-214936) therapy in patients with advanced renal cell carcinoma. *Br. J. Cancer* **96**, 567–574 (2007).
16. M. Hashimoto, K. Araki, M. A. Cardenas, P. Li, R. R. Jadhav, H. T. Kissick, W. H. Hudson, D. J. McGuire, R. C. Obeng, A. Wieland, J. Lee, D. T. McManus, J. L. Ross, S. J. Im, J. Lee, J. X. Lin, B. Hu, E. E. West, C. D. Scharer, G. J. Freeman, A. H. Sharpe, S. S. Ramalingam, A. Pellerin, V. Teichgräber, W. J. Greenleaf, C. Klein, J. J. Goronzy, P. Umaña, W. J. Leonard, K. A. Smith, R. Ahmed, PD-1 combination therapy with IL-2 modifies CD8(+) T cell exhaustion program. *Nature* **610**, 173–181 (2022).
17. P. Vantourout, J. Eum, M. C. Poole, T. S. Hayday, A. G. L. Laing, K. Hussain, R. Nuamah, S. Kannambath, J. M. Moisan, A. Stoop, S. Battaglia, R. Servattalab, J. Hsu, A. Bayliffe, M. Katragadda, A. C. Hayday, Innate TCRβ-chain engagement drives human T cells toward distinct memory-like effector states. *Sci. Immunol.* **3**, eaas9103 (2023).
18. K. Hussain, P. Vantourout, M. Poole, J. E. Eum, T. Hayday, A. Laing, S. Battaglia, M. Katragadda, J. Lowry, J. Hsu, A. Hayday, An atypical central memory like phenotype can be induced in human T cells by Innate TCRαβ engagement. *J. Immunother. Cancer* **10**, A1447 (2022).
19. P. V. Sivakumar, R. Garcia, K. S. Waggie, M. Anderson-Haley, A. Nelson, S. D. Hughes, Comparison of vascular leak syndrome in mice treated with IL21 or IL2. *Comp. Med.* **63**, 13–21 (2013).
20. J. W. Yu, S. Bhattacharya, N. Yanamandra, D. Kilian, H. Shi, S. Yadavilli, Y. Katlinskaya, H. Kaczynski, M. Conner, W. Benson, A. Hahn, L. Seestaller-Wehr, M. Bi, N. J. Vitali, L. Tsvetkov, W. Halsey, A. Hughes, C. Traini, H. Zhou, J. Jing, T. Lee, D. J. Figueroa, S. Brett, C. B. Hopson, J. F. Smothers, A. Hoos, R. Srinivasan, Tumor-immune profiling of murine syngeneic tumor models as a framework to guide mechanistic studies and predict therapy response in distinct tumor microenvironments. *PLOS ONE* **13**, e0206223 (2018).
21. O. Khan, J. R. Giles, S. McDonald, S. Manne, S. F. Ngiow, K. P. Patel, M. T. Werner, A. C. Huang, K. A. Alexander, J. E. Wu, J. Attanasio, P. Yan, S. M. George, B. Bengsch, R. P. Staupe, G. Donahue, W. Xu, R. K. Amaravadi, X. Xu, G. C. Karakousis, T. C. Mitchell, L. M. Schuchter, J. Kaye, S. L. Berger, E. J. Wherry, TOX transcriptionally and epigenetically programs CD8(+) T cell exhaustion. *Nature* **571**, 211–218 (2019).
22. X. Liu, Y. Wang, H. Lu, J. Li, X. Yan, M. Xiao, J. Hao, A. Alekseev, H. Khong, T. Chen, R. Huang, J. Wu, Q. Zhao, Q. Wu, S. Xu, X. Wang, W. Jin, S. Yu, Y. Wang, L. Wei, A. Wang, B. Zhong, L. Ni, X. Liu, R. Nurieva, L. Ye, Q. Tian, X. W. Bian, C. Dong, Genome-wide analysis identifies NR4A1 as a key mediator of T cell dysfunction. *Nature* **567**, 525–529 (2019).
23. N. Weisshaar, J. Wu, Y. Ming, A. Madi, A. Hotz-Wagenblatt, S. Ma, A. Mieg, M. Hering, F. Zettl, K. Mohr, T. Schlimbach, N. Ten Bosch, F. Hertel, L. Müller, H. Byren, M. Wang, H. Borgers, M. Munz, L. Schmitt, F. van der Hoeven, U. Kloz, R. Carretero, N. Schleußner, R. F. Jackstadt, I. Hofmann, G. Cui, Rgs16 promotes antitumor CD8(+) T cell exhaustion. *Sci. Immunol.* **7**, eabh1873 (2022).
24. G. Petkau, T. J. Mitchell, K. Chakraborty, S. E. Bell, V. D. Angeli, L. Matheson, D. J. Turner, A. Saveliev, O. Gizlenci, F. Salerno, P. D. Katsikis, M. Turner, The timing of differentiation and

potency of CD8 effector function is set by RNA binding proteins. *Nat. Commun.* **13**, 2274 (2022).
25. D. Mori, C. Grégoire, G. Voisinne, J. Celis-Gutierrez, R. Aussel, L. Girard, M. Camus, M. Marcellin, J. Argenty, O. Burlet-Schiltz, F. Fiore, A. Gonzalez de Peredo, M. Malissen, R. Roncagalli, B. Malissen, The T cell CD6 receptor operates a multitask signalosome with opposite functions in T cell activation. *J. Exp. Med.* **218**, e20201011 (2021).
26. X. Wen, H. Liu, G. Xiao, X. Liu, Downregulation of the transcription factor KLF4 is required for the lineage commitment of T cells. *Cell Res.* **21**, 1701–1710 (2011).
27. L. Codarri Deak, V. Nicolini, M. Hashimoto, M. Karagianni, P. C. Schwalie, L. Lauener, E. M. Varypataki, M. Richard, E. Bommer, J. Sam, S. Joller, M. Perro, F. Cremasco, L. Kunz, E. Yanguez, T. Hüsser, R. Schlenker, M. Mariani, V. Tosevski, S. Herter, M. Bacac, I. Waldhauer, S. Colombetti, X. Gueripel, S. Wullschleger, M. Tichet, D. Hanahan, H. T. Kissick, S. Leclair, A. Freimoser-Grundschober, S. Seeber, V. Teichgräber, R. Ahmed, C. Klein, P. Umaña, PD-1-cis IL-2R agonism yields better effectors from stem-like CD8(+) T cells. *Nature* **610**, 161–172 (2022).
28. M. Stringhini, P. Probst, D. Neri, Immunotherapy of CT26 murine tumors is characterized by an oligoclonal response of tissue-resident memory T cells against the AH1 rejection antigen. *Eur. J. Immunol.* **50**, 1591–1597 (2020).
29. N. P. Rudqvist, K. A. Pilones, C. Lhuillier, E. Wennerberg, J. W. Sidhom, R. O. Emerson, H. S. Robins, J. Schneck, S. C. Formenti, S. Demaria, Radiotherapy and CTLA-4 blockade shape the TCR repertoire of tumor-infiltrating T cells. *Cancer Immunol. Res.* **6**, 139–150 (2018).
30. P. Deegen, O. Thomas, O. Nolan-Stevaux, S. Li, J. Wahl, P. Bogner, F. Aeffner, M. Friedrich, M. Z. Liao, K. Matthes, D. Rau, B. Rattel, T. Raum, P. Kufer, A. Coxon, J. M. Bailis, The PSMA-targeting half-life extended BiTE therapy AMG 160 has potent antitumor activity in preclinical models of metastatic castration-resistant prostate cancer. *Clin. Cancer Res.* **27**, 2928–2937 (2021).
31. P. J. Engelberts, I. H. Hiemstra, B. de Jong, D. H. Schuurhuis, J. Meesters, I. Beltran Hernandez, S. C. Oostindie, J. Neijssen, E. N. van den Brink, G. J. Horbach, S. Verploegen, A. F. Labrijn, T. Salcedo, J. Schuurman, P. Parren, E. C. W. Breij, DuoBody-CD3xCD20 induces potent T-cell-mediated killing of malignant B cells in preclinical models and provides opportunities for subcutaneous dosing. *EBioMedicine* **52**, 102625 (2020).
32. F. Van Gool, A. B. Molofsky, M. M. Morar, M. Rosenzwajg, H. E. Liang, D. Klatzmann, R. M. Locksley, J. A. Bluestone, Interleukin-5-producing group 2 innate lymphoid cells control eosinophilia induced by interleukin-2 therapy. *Blood* **124**, 3572–3576 (2014).
33. D. Skokos, J. C. Waite, L. Haber, A. Crawford, A. Hermann, E. Ullman, R. Slim, S. Godin, D. Ajithdoss, X. Ye, B. Wang, Q. Wu, I. Ramos, A. Pawashe, L. Canova, K. Vazzana, P. Ram, E. Herlihy, H. Ahmed, E. Oswald, J. Golubov, P. Poon, L. Havel, D. Chiu, M. Lazo, K. Provoncha, K. Yu, J. Kim, J. J. Warsaw, N. Stokes Oristian, C. J. Siao, D. Dudgeon, T. Huang, T. Potocky, J. Martin, D. MacDonald, A. Oyejide, A. Rafique, W. Poueymirou, J. R. Kirshner, E. Smith, W. Olson, J. Lin, G. Thurston, M. A. Sleeman, A. J. Murphy, G. D. Yancopoulos, A class of costimulatory CD28-bispecific antibodies that enhance the antitumor activity of CD3-bispecific antibodies. *Sci. Transl. Med.* **12**, eaaw7888 (2020).
34. T. W. Chang, P. C. Kung, S. P. Gingras, G. Goldstein, Does OKT3 monoclonal antibody react with an antigen-recognition structure on human T cells? *Proc. Natl. Acad. Sci. U.S.A.* **78**, 1805–1808 (1981).
35. A. L. Lanz, G. Masi, N. Porciello, A. Cohnen, D. Cipria, D. Prakaash, Š. Bálint, R. Raggiaschi, D. Galgano, D. K. Cole, M. Lepore, O. Dushek, M. L. Dustin, M. S. P. Sansom, A. C. Kalli, O. Acuto, Allosteric activation of T cell antigen receptor signaling by quaternary structure relaxation. *Cell Rep.* **36**, 109531 (2021).
36. V. Gopalakrishnan, C. N. Spencer, L. Nezi, A. Reuben, M. C. Andrews, T. V. Karpinets, P. A. Prieto, D. Vicente, K. Hoffman, S. C. Wei, A. P. Cogdill, L. Zhao, C. W. Hudgens, D. S. Hutchinson, T. Manzo, M. P. de Macedo, T. Cotechini, T. Kumar, W. S. Chen, S. M. Reddy, R. S. Sloane, J. Galloway-Pena, H. Jiang, P. L. Chen, E. J. Shpall, K. Rezvani, A. M. Alousi, R. F. Chemaly, S. Shelburne, L. M. Vence, P. C. Okhuysen, V. B. Jensen, A. G. Swennes, F. McAllister, E. M. R. Sanchez, Y. Zhang, E. Le Chatelier, L. Zitvogel, N. Pons, J. L. Austin-Breneman, L. E. Haydu, E. M. Burton, J. M. Gardner, E. Sirmans, J. Hu, A. J. Lazar, T. Tsujikawa, A. Diab, H. Tawbi, I. C. Glitza, W. J. Hwu, S. P. Patel, S. E. Woodman, R. N. Amaria, M. A. Davies, J. E. Gershenwald, P. Hwu, J. E. Lee, J. Zhang, L. M. Coussens, Z. A. Cooper, P. A. Futreal, C. R. Daniel, N. J. Ajami, J. F. Petrosino, M. T. Tetzlaff, P. Sharma, J. P. Allison, R. R. Jenq, J. A. Wargo, *Science* **359**, Gut microbiome modulates response to anti-PD-1 immunotherapy in melanoma patients, 97–Gut microbiome modulates response to anti-PD-1 immunotherapy in melanoma patie103 (2018).
37. L. F. Mager, R. Burkhard, N. Pett, N. C. A. Cooke, K. Brown, H. Ramay, S. Paik, J. Stagg, R. A. Groves, M. Gallo, I. A. Lewis, M. B. Geuking, K. D. McCoy, Microbiome-derived inosine modulates response to checkpoint inhibitor immunotherapy. *Science* **369**, 1481–1489 (2020).
38. K. M. Knudson, K. C. Hicks, X. Luo, J. Q. Chen, J. Schlom, S. R. Gameiro, M7824, a novel bifunctional anti-PD-L1/TGFβ Trap fusion protein, promotes anti-tumor efficacy as monotherapy and in combination with vaccine. *Oncoimmunology* **7**, e1426519 (2018).
39. C. D. Slade, K. L. Reagin, H. G. Lakshmanan, K. D. Klonowski, W. T. Watford, Placenta-specific 8 limits IFNγ production by CD4 T cells in vitro and promotes establishment of influenza-specific CD8 T cells in vivo. *PLOS ONE* **15**, e0235706 (2020).
40. L. M. Snell, W. Xu, D. Abd-Rabbo, G. Boukhaled, M. Guo, B. L. Macleod, H. J. Elsaesser, K. Hezaveh, N. Alsahafi, S. Lukhele, S. Nejat, R. Prabhakaran, S. Epelman, T. L. McGaha, D. G. Brooks, Dynamic CD4(+) T cell heterogeneity defines subset-specific suppression and PD-L1-blockade-driven functional restoration in chronic infection. *Nat. Immunol.* **22**, 1524–1537 (2021).
41. R. R. Jadhav, S. J. Im, B. Hu, M. Hashimoto, P. Li, J. X. Lin, W. J. Leonard, W. J. Greenleaf, R. Ahmed, J. J. Goronzy, Epigenetic signature of PD-1+ TCF1+ CD8 T cells that act as resource cells during chronic viral infection and respond to PD-1 blockade. *Proc. Natl. Acad. Sci. U.S.A.* **116**, 14113–14118 (2019).
42. S. Makita, H. Takatori, H. Nakajima, Post-transcriptional regulation of immune responses and inflammatory diseases by RNA-binding ZFP36 family proteins. *Front. Immunol.* **12**, 711633 (2021).
43. B. Liu, X. Hu, K. Feng, R. Gao, Z. Xue, S. Zhang, Y. Zhang, E. Corse, Y. Hu, W. Han, Z. Zhang, Temporal single-cell tracing reveals clonal revival and expansion of precursor exhausted T cells during anti-PD-1 therapy in lung cancer. *Nat. Cancer* **3**, 108–121 (2022).
44. K. E. Yost, A. T. Satpathy, D. K. Wells, Y. Qi, C. Wang, R. Kageyama, K. L. McNamara, J. M. Granja, K. Y. Sarin, R. A. Brown, R. K. Gupta, C. Curtis, S. L. Bucktrout, M. M. Davis, A. L. S. Chang, H. Y. Chang, Clonal replacement of tumor-specific T cells following PD-1 blockade. *Nat. Med.* **25**, 1251–1259 (2019).
45. E. B. Day, C. Guillonneau, S. Gras, N. L. La Gruta, D. A. Vignali, P. C. Doherty, A. W. Purcell, J. Rossjohn, S. J. Turner, Structural basis for enabling T-cell receptor diversity within biased virus-specific CD8+ T-cell responses. *Proc. Natl. Acad. Sci. U.S.A.* **108**, 9536–9541 (2011).
46. K. Gao, L. Chen, Y. Zhang, Y. Zhao, Z. Wan, J. Wu, L. Lin, Y. Kuang, J. Lu, X. Zhang, L. Tian, X. Liu, X. Qiu, Germline-encoded TCR-MHC contacts promote TCR V gene bias in umbilical cord blood T cell repertoire. *Front. Immunol.* **10**, 2064 (2019).
47. T. Guo, M. Y. Koo, Y. Kagoya, M. Anczurowski, C. H. Wang, K. Saso, M. O. Butler, N. Hirano, A subset of human autoreactive CD1c-restricted T cells preferentially expresses TRBV4-1(+) TCRs. *J. Immunol.* **200**, 500–511 (2018).
48. D. K. Cole, F. Yuan, P. J. Rizkallah, J. J. Miles, E. Gostick, D. A. Price, G. F. Gao, B. K. Jakobsen, A. K. Sewell, Germ line-governed recognition of a cancer epitope by an immunodominant human T-cell receptor. *J. Biol. Chem.* **284**, 27281–27289 (2009).
49. G. C. Wang, P. Dash, J. A. McCullers, P. C. Doherty, P. G. Thomas, T cell receptor αβ diversity inversely correlates with pathogen-specific antibody levels in human cytomegalovirus infection. *Sci. Transl. Med.* **4**, 128ra142 (2012).
50. I. Grenga, R. N. Donahue, L. M. Lepone, J. Richards, J. Schlom, A fully human IgG1 anti-PD-L1 MAb in an in vitro assay enhances antigen-specific T-cell responses. *Clin. Transl. Immunol.* **5**, e83 (2016).

Acknowledgments: We thank P. Hernandez (Vivia Biotech) for investigating the baseline frequencies for Vβ6-5 in various patients with cancer, S. Battaglia and H. Hassan (Bridge Informatics) for assisting in single-cell sequencing analysis, D. Weingarten (NIH) for editorial assistance in the preparation of this manuscript, S. Kharkwal for setting up the murine tumor antigen recall experiment, and R. Ruidera for flow cytometry support. **Funding:** This work was supported by the Intramural Program of the Center for Cancer Research of the National Cancer Institute (NCI), National Institutes of Health, and an NCI Cooperative Research and Development Agreement (CRADA) with Marengo Therapeutics. **Author contributions:** J.H., M.K., and A.B. conceived the concept. J.H., R.N.D., J.L., W.H., G.G., K.S., J.T., R.S., and Y.-T.T. performed the experiments. G.G. and R.S. performed molecule development and characterization. J.H., R.N.D., J.L., J.T., and Y.-T.T. performed in vitro assays. W.H. performed in vivo mouse studies. J.H. and A.S. performed scRNA-seq and TCR analyses. K.S. performed nonhuman primate studies. J.H., R.N.D., J.M., Y.-T.T., M.K., S.P., J.S., and A.B. analyzed the data. J.H., A.B., R.N.D., J.M., J.S., and A.S. wrote the manuscript. A.S., R.C., K.L., E.J.W., Z.S., and J.L.G. provided technical support, manuscript review, and conceptual advice. **Competing interests:** J.H., M.K., A.B., J.L., W.H., G.G., K.S., J.T., R.S., K.L., and Z.S. are employees of Marengo Therapeutics and own stock in the company. R.C. is a member of the board of directors of Marengo Therapeutics and owns stock in the company. A. S. has a consulting agreement in place with Marengo Therapeutics. R.N.D., Y.-T.T., J.S., and J.L.G. report that their institute (NCI) has a Cooperative Research and Development Agreement (CRADA) with Marengo Therapeutics. J.H., M.K., G.G., and S.P. are inventors on patent applications US63/172,468 and PCT/US2022/023922 held/submitted by Marengo Therapeutics that cover anti-TCRVβ × Cytokine. E.J.W. is a member of the Parker Institute for Cancer Immunotherapy and has consulting agreements with or is on the scientific advisory board for Merck, Roche, Pieris, Marengo Therapeutics, and Surface Oncology. E.J.W. has a patent licensing agreement on the PD-1 pathway with Roche-Genentech and is a founder of Arsenal Biosciences. J.L.G. as part of his official duties is an uncompensated co-chair of the scientific advisory board for Marengo Therapeutics. **Data and materials availability:** All data associated with this study are present in the paper or the Supplementary Materials. scRNA-seq data are available from the NCBI Gene Expression Omnibus database (GSE223311). Code and newly

created data sets used to analyze the data are available at Zenodo DOI:10.5281/zenodo.10011622 and Zenodo DOI:10.5281/zenodo.10028250 for analysis from published datasets. Marengo materials described in this manuscript [STAR0602, mSTAR1302, anti-Vβ6/Vβ10 (including the flow reagent and Fc-enabled version), IL-2 controls, and isotype controls] will be made available to qualified, academic, noncommercial researchers through a material transfer agreement upon request to A.B. at Marengo Therapeutics.

Submitted 29 March 2023
Resubmitted 20 July 2023
Accepted 27 October 2023
Published 29 November 2023
10.1126/scitranslmed.adi0258

Science Translational Medicine

A T cell receptor # chain–directed antibody fusion molecule activates and expands subsets of T cells to promote antitumor activity

Jonathan Hsu, Renee N. Donahue, Madan Katragadda, Jessica Lowry, Wei Huang, Karunya Srinivasan, Gurkan Guntas, Jian Tang, Roya Servattalab, Jacques Moisan, Yo-Ting Tsai, Allart Stoop, Sangeetha Palakurthi, Raj Chopra, Ke Liu, E. John Wherry, Zhen Su, James L. Gulley, Andrew Bayliffe, and Jeffrey Schlom

Sci. Transl. Med. **15** (724), eadi0258. DOI: 10.1126/scitranslmed.adi0258